

RESOURCE ALLOCATION IN DS-CDMA SYSTEMS WITH
SIDE INFORMATION AT THE TRANSMITTER

A Dissertation

by

BEMINI HENNADIGE JANATH PEIRIS

Submitted to the Office of Graduate Studies of
Texas A&M University
in partial fulfillment of the requirements for the degree of

DOCTOR OF PHILOSOPHY

December 2006

Major Subject: Electrical Engineering

RESOURCE ALLOCATION IN DS-CDMA SYSTEMS WITH
SIDE INFORMATION AT THE TRANSMITTER

A Dissertation

by

BEMINI HENNADIGE JANATH PEIRIS

Submitted to the Office of Graduate Studies of
Texas A&M University
in partial fulfillment of the requirements for the degree of
DOCTOR OF PHILOSOPHY

Approved by:

| | |
|-------------------------|---|
| Co-Chairs of Committee, | Krishna R. Narayanan Scott L. Miller |
| Committee Members, | Costas N. Georgiades Narasimha R. Reddy G. Donald Allen |
| Head of Department, | Costas N. Georgiades |

December 2006

Major Subject: Electrical Engineering

ABSTRACT

Resource Allocation in DS-CDMA Systems with
Side Information at the Transmitter. (December 2006)

Bemini Hennadige Janath Peiris, B.Sc., University of Moratuwa, Sri Lanka;
M.Eng., Asian Institute of Technology, Thailand

Co-Chairs of Advisory Committee: Dr. Krishna R. Narayanan
Dr. Scott L. Miller

In a multiuser DS-CDMA system with frequency selectivity, each user's spreading sequence is transmitted through a different channel and the autocorrelation and the cross correlation properties of the received sequences will not be the same as that of the transmitted sequences. The best way of designing spreading sequences for frequency selective channels is to design them at the receiver exploiting the users' channel characteristics. By doing so, we can show that the designed sequences outperform single user AWGN performance.

In existing sequence design algorithms for frequency selective channels, the design is done in the time domain and the connection to frequency domain properties is not established. We approach the design of spreading sequences based on their frequency domain characteristics. Based on the frequency domain characteristics of the spreading sequences with unconstrained amplitudes and phases, we propose a reduced-rank sequence design algorithm that reduces the computational complexity, feedback bandwidth and improves the performance of some existing sequence design algorithms proposed for frequency selective channels.

We propose several different approaches to design the spreading sequences with

constrained amplitudes and phases for frequency selective channels. First, we use the frequency domain characteristics of the unconstrained spreading sequences to find a set of constrained amplitude sequences for a given set of channels. This is done either by carefully assigning an already existing set of sequences for a given set of users or by mapping unconstrained sequences onto a unit circle. Secondly, we use an information theoretic approach to design the spreading sequences by matching the spectrum of each user's sequence to the water-filling spectrum of the user's channel.

Finally, the design of inner shaping codes for single-head and multi-head magnetic recoding channels is discussed. The shaping sequences are designed considering them as short spreading codes matched to the recoding channels. The outer channel code is matched to the inner shaping code using the extrinsic information transfer chart analysis.

In this dissertation we introduce a new frequency domain approach to design spreading sequences for frequency selective channels. We also extend this proposed technique to design inner shaping codes for partial response channels.

To my wife Dilani

ACKNOWLEDGMENTS

I would like to express my sincere gratitude to my Ph.D. co-adviser, Dr. Krishna R. Narayanan, for his stimulating suggestions and constant encouragement. His wide knowledge and his logical way of thinking have been of great value to me. I admire his kindness and intelligence. It is a great honor for me to conduct this dissertation under his supervision.

I use this opportunity to thank my co-advisor Dr. Scott L. Miller. His insights into technical matters and constant discussions helped me to achieve this goal. Without his encouragement and constant guidance, I could not have finished this dissertation.

I also use this opportunity to thank the committee members, Dr. Costas Georgiades, Dr. Narasimha Reddy and Dr. G. Donald Allen, who have always been supportive of my work. Special thanks to them for their constructive comments and advice on my research. Their ideas and concepts have had a remarkable influence on my research.

I would like to thank my friends from the Wireless Communications Laboratory, Abhiram, Anant, Doan, Hari, Jing, Kai Shi, Kapil, Linja, Makesh, Nitin and Vivek, for fruitful discussions and help during my stay in College Station.

Special thanks go to professors in the Wireless Communications group for their excellent teaching. I have learned much more from both course work and the process of doing research.

Many thanks go to my financial supporter: National Science Foundation (NSF), from which my Ph.D. adviser has generously provided me support for the entire time of my study at TAMU.

Heartfelt thanks go to my wife Dilani Peiris for her constant love, encourage-

ment and support. My parents deserve the most credit for their nurturing, love and patience. It would be impossible to follow this long term of study without their support.

TABLE OF CONTENTS

| CHAPTER | | Page |
|---------|--|------|
| I | INTRODUCTION | 1 |
| II | BACKGROUND | 8 |
| | A. System model | 8 |
| | B. Multiuser detectors in a DS-CDMA system | 10 |
| | 1. De-correlator detector | 11 |
| | 2. MMSE detector | 11 |
| | 3. Successive interference cancellation | 12 |
| | 4. Turbo codes | 14 |
| | 5. Low density parity check codes | 16 |
| | 6. Extrinsic information transfer chart | 17 |
| III | A SPECTRAL DOMAIN APPROACH TO DESIGN SPREAD- ING SEQUENCES FOR FREQUENCY SELECTIVE FAD- ING CHANNELS | 19 |
| | A. Background | 19 |
| | B. Frequency domain characteristics of good spreading sequences | 21 |
| | C. Designing of spreading sequences with unconstrained amplitudes and phases in the frequency domain | 27 |
| | 1. Main idea | 27 |
| | 2. Proposed modification to the approach in [32] | 28 |
| | a. Computational complexity | 33 |
| | b. Required feedback bandwidth | 34 |
| | 3. The proposed modification for an existing signa- ture sequence optimization scheme | 34 |
| | a. Transmitter and spreading sequence optimiza- tion scheme | 34 |
| | b. Signature sequence optimization based on MMSE criteria | 37 |
| IV | THE DESIGN OF CONSTRAINED AMPLITUDE SPREAD- ING SEQUENCES USING SPECTRAL DOMAIN PROP- ERTIES | 43 |

| CHAPTER | | Page |
|---------|---|------|
| | A. Constrained amplitude sequence design | 45 |
| | 1. Constrained amplitude sequence design by map- ping unconstrained sequences onto a unit circle | 45 |
| | 2. The design of constrained amplitude sequences us- ing already existing family of sequences | 48 |
| V | THE DESIGN OF FINITE ALPHABET SPREADING SE- QUENCES BASED ON THE WATERFILLING CONCEPT . . | 53 |
| | A. Design of spreading sequences | 53 |
| | 1. Basic idea | 54 |
| | 2. Single user design | 55 |
| | 3. Selection of the optimal short spreading sequences . . | 58 |
| | 4. Long spreading codes with channel coding | 61 |
| | B. Receiver structure | 62 |
| VI | THE DESIGN OF SHAPING CODES FOR PARTIAL RE- SPONSE CHANNELS | 66 |
| | A. Background | 67 |
| | B. The design of shaping codes for single-track magnetic recording systems | 69 |
| | C. The design of shaping codes for a multi-track magnetic recording systems | 73 |
| | 1. The design of shaping codes for two-track magnetic recording systems | 74 |
| | D. Two-track system with suboptimal decoding | 78 |
| | E. Simulation results | 81 |
| VII | CONCLUSIONS | 84 |
| | REFERENCES | 86 |
| | APPENDIX A | 93 |
| | VITA | 95 |

LIST OF FIGURES

| FIGURE | | Page |
|--------|---|------|
| 1 | Block diagram of a synchronous uplink DS-CDMA system. | 9 |
| 2 | Block diagram of a multiuser detector. | 12 |
| 3 | Block diagram of a turbo encoder. | 14 |
| 4 | Block diagram of a turbo decoder. | 15 |
| 5 | Graph structure of an LDPC code. | 16 |
| 6 | Power spectrum of each user's spreading sequence. | 22 |
| 7 | Power spectrum of each user's spreading sequence. Only four of the users' sequences' spectra and channels' spectra are shown. | 23 |
| 8 | Cumulative Density Functions (CDFs) of the transmitted and the received power of users' spreading sequences. | 25 |
| 9 | Performance comparison of the two reduced-rank optimization schemes. RH=Rajappan and Honig algorithm [32]. | 31 |
| 10 | Performance comparison of the two reduced-rank optimization schemes. RH=Rajappan and Honig algorithm [32]. $K=12$, $N=16$ and $L=2$ | 32 |
| 11 | Performance comparison of the transmitter power and spreading sequence optimization scheme [10] with the proposed reduced- rank version of it. CU=Concha and Ulukus [10]. $K=8$, $N=5$ and $L=2$. $\frac{1}{\sigma^2}=5$ dB. | 39 |
| 12 | Performance comparison of the transmitter power and spreading sequence optimization scheme [10] with the proposed reduced- rank version of it. CU=Concha and Ulukus [10]. $K=12$, $N=16$ and $L=2$. $\frac{1}{\sigma^2}=5$ dB. | 40 |

| FIGURE | | Page |
|--------|--|------|
| 13 | Performance comparison of MMSE sequence optimization scheme [10] with the proposed reduced-rank version of it. CU=Concha and Ulukus [10]. Uplink is considered. $K=12$, $N=16$ and $L=2$ | 41 |
| 14 | Performance comparison of MMSE sequence optimization scheme [10] with the proposed reduced-rank version of it. CU=Concha and Ulukus [10]. Downlink is considered. $K=12$, $N=16$ and $L=2$. . . | 42 |
| 15 | PAPR distributions of single code and multi-code DS-CDMA signals. | 43 |
| 16 | The performance of the unit circle sequences with frequency domain quantized coefficients. $K=12$, $N=16$. RH-quantized = Sequences designed according to (3.13) with quantized $\alpha_{k,r}$. RH-unquantized = Sequences designed according to (3.13) with unquantized $\alpha_{k,r}$ and $D = N$ | 46 |
| 17 | Performance of the Oppermann sequences. $K=12$, $N=15$. Uplink is considered. | 50 |
| 18 | Comparison of the waterfilling spectrum with the spectrum of the complex sequence generated by an appropriate first order Markov chain. | 58 |
| 19 | Figure that illustrates the selection procedure of short spreading sequences from the long Markov sequence. | 59 |
| 20 | Flow chart to find a set of spreading sequences with low cross correlation properties. | 60 |
| 21 | BER performance comparison of the system with short codes. $N=16$, $K=12$ | 63 |
| 22 | BER performance comparison of the system with long codes [41]. $K=5$, $N=16$ | 64 |
| 23 | i.u.d. capacity dicode channel with bi-phase coding vs i.u.d. capacity of dicode channel. | 70 |
| 24 | Trellis section with assigned shaping codes. | 71 |
| 25 | Capacity of the scheme with parallel branches. Rate= $2/3$ | 72 |

| FIGURE | | Page |
|--------|--|------|
| 26 | Fractional capacity loss due to the combining of two channels. | 75 |
| 27 | The EXIT chart for the two-track magnetic recording channel with individually optimized sequences. Optimum combined decoding assumed. Inner code rate is 0.25 bits/sample. | 76 |
| 28 | The EXIT chart for two-track channel with jointly optimized sequences. Optimum combined decoding is assumed. Inner code rate is 0.25 b/sample. | 77 |
| 29 | Per-user channel capacity for different shaping codes. Each track's channel is $1 - D$ | 79 |
| 30 | BER performance with different shaping codes. $N=40,000$, overall rate is 0.125. Rate LDPC=0.50. | 81 |
| 31 | BER performance with different shaping codes. $N=40,000$, overall rate is 0.0625. Rate LDPC=0.25. | 82 |

CHAPTER I

INTRODUCTION

Today, the wireless communication industry is one of the fastest growing fields in the communication industry and there is an increasing demand from the customers for the radio system resources. To satisfy the customers' requirements, the communication system designers have to design the systems such that the system resources are used most efficiently and at a low cost. Further, the wireless communication systems are mostly multiuser systems and the limited system resources should be carefully shared among the users.

In most of the systems, user specific signals are separated either in time domain (time division multiple access, TDMA), frequency domain (frequency division multiple access, FDMA) or in code domain (code division multiple access, CDMA). In TDMA or FDMA schemes, the decoder can simply recover the users' information by decoding the information corresponding to each user's specified time or frequency slot. But, in a CDMA system, users are allowed to share the bandwidth and time resources by transmitting simultaneously over the same band. In this case, each user's information is encoded using a user specific signature sequence. However, at the receiver, each user's information is recovered by simply despreading the received signal using that user's spreading sequence. But, since the received signal is a linear combination of all the user's transmitted signals, each user's decoded signal could be subjected to a heavy interference from the other users' signals in the system, if the spreading sequences are arbitrarily designed. The reduction of the interference from the other users is usually handled through a careful design of spreading sequences.

The journal model is *IEEE Transactions on Automatic Control*.

Precisely, when the received signal is corrupted only by additive white Gaussian noise (AWGN), the signature sequences should be designed such that the sum of squared cross correlation among the users' spreading sequences is minimized [1].

The capacity of direct sequence code division multiple access (DS-CDMA) systems for additive white Gaussian noise channels has been studied extensively in literature [2]-[3]. In [2], Rupf and Massey have derived the capacity region of a single cell synchronous CDMA system for a given set of spreading sequences. There, they have shown that the sum rate of a DS-CDMA system with equal power users can be maximized by designing the spreading sequences to be orthogonal to each other when the number of users is less than or equal to the spreading length. If the number of users is greater than the spreading length, the sequences should be designed to achieve the Welch bound with equality (WBE). In the latter scenario, sum rate of the multiuser system is equal to the sum capacity of the system.

In [3], Viswanath et al. have defined the user capacity of a CDMA cell as the maximum number of users per unit spreading length admissible in the system such that each user has a given signal to interference ratio (SIR). They have defined the admissibility of K users for the system with spreading length N , power constraint P and each having certain SIR requirement as being able to find signature sequence and a power for each and every user such that each user achieves the target SIR. Existence of these sequences were also proved and shown that the sequences are orthogonal when $K < N$ and achieves Welch bound when $K > N$, hence the information theoretic sum capacity of the system.

In literature, there have been many attempts to find practical algorithms to design spreading sequences for DS-CDMA systems [4]-[7]. In [4], Ulukus and Yates have proposed an iterative algorithm that updates transmitter signature sequences sequentially in a distributed fashion. At each step of the algorithm, each user's

signature sequence is replaced by the minimum mean squared error (MMSE) receiver designed for that particular user. By doing so, they have shown that the sum of squared cross correlations among the users' spreading sequences is minimized at each user's iteration. They have also shown that, when the number of users is greater than the spreading length, the Welch bound equality can be obtained. In [5], Rajappan and Honig also have shown a similar iterative algorithm to design the spreading sequences based on the Lagrangian optimization technique.

While [4]-[7] consider the spreading sequence designs for frequency flat fading channels, practical wireless channels are often notoriously dispersive and this dispersion leads to intersymbol interference (ISI) where the energy of a given symbol spills over into the adjacent symbols. Due to this phenomena, it is not sufficient to minimize the sum of squared correlations among the spreading sequences for frequency selective channels. This is because, in a frequency selective channel, each user's spreading sequence is transmitted through a different frequency selective channel and the correlation properties of the filtered spreading sequences may be different from that of the transmitted spreading sequences. In a DS-CDMA system, it is a common practice to use a RAKE receiver which attempts to collect the energy from all the paths that the transmitted signal follows. The RAKE receiver requires the knowledge of the channel coefficients to perform the maximal ratio combining of the signals coming from different paths with different gains and phase shifts. Since the receiver has access to the channel state information, it is desirable to use these estimated channel coefficients to design a set of spreading sequences that is best suited for a particular set of channels. The objective here is to exploit the channel state information and design a set of sequences to maximize the ratio between each user's received power and the interference plus noise at the receiver.

The design of signature sequences for frequency selective channels has received

some attention only recently. Jang and Vojcic [8] proposed a transmitter precoding technique to reduce the multiple access and inter-chip interference (ICI). Rajappan and Honig [9] proposed a technique for joint transmitter and receiver adaptation for multipath inter-symbol interference channels. Using this technique, for the uplink, they have shown that near single user performance can be achieved. In [10], Concha and Uluks have considered the optimization of spreading sequences with multipath fading under the constraint that each user requires a target signal to interference plus noise ratio (SINR). It is worthwhile to note that, although some of the existing techniques such as [8]-[11] use adaptive algorithms for the maximization of the sum rate of the system, most of those efforts are based on designing spreading sequences in time domain and the connection to frequency domain characteristics of spreading sequences is not made.

In this dissertation, we embark the journey to find whether we can get some insight into the design of the spreading sequences by looking into the frequency domain characteristics of well designed spreading sequences. Based on the frequency domain properties of the well-designed sequences, we propose to design the sequences for frequency selective channels with reasonably less computational complexity and feedback bandwidth.

In most of the existing algorithms which have been proposed for frequency selective channels, the spreading sequences are assumed to have constrained amplitudes and phases. This demands high feedback bandwidth to transmit the designed sequences from the designed end (transmitter/receiver) to the other end (receiver/transmitter). The other difficulty of using unconstrained sequences is that, at the mobile unit, the peak to average power ratio could be very high. This demands considerably large power amplifier dynamic range increasing the cost of the transmitter amplifier. Hence, the design of constrained amplitude spreading sequences is a

demanding task.

In [12] and [13], Krishnamurthy et al. have proposed a discrete stochastic optimization technique to adaptively optimize the signature sequences employing a minimum mean square receivers for slowly time-varying channels. The method is a global optimization technique for discrete alphabets where the algorithm try to optimize the global cost function which is the sum of signal to noise plus interference ratio values of all the active users in the system. Unfortunately, the computational complexity of this algorithm increases exponentially with the spreading length and the number of users. Hence, for a practical system, this method is too computationally complex to be incorporated. Instead, In this dissertation, we propose three new approaches to design constrained amplitude spreading sequences for slowly time-varying frequency selective channels. The main advantage of our scheme over the scheme proposed in [12] is that our proposed algorithm provides a set of sequences for slowly time-varying channels that performs very close to that of the scheme proposed in [12] with much reduced complexity.

In the first approach, we apply the Lagrangian relaxation method on existing sequence design algorithms to design the constrained alphabet sequences. In the second method, we use the knowledge of the frequency domain characteristics of the well-designed unconstrained spreading sequences and carefully assign existing set of narrow-band spreading sequences to maximize the system performance which is the SINR. Finally, we assume that the spreading sequences are a set of low rate channel codes and we design the spreading sequences to maximize the single user information rate while minimizing the cross correlation among the users.

Since the introduction of magnetic tape recording 50 years ago, the magnetic recording devices play an important role of recording vast amounts of data and retrieving the stored data very quickly [14]. Today, hard disk drives have become the

most common form of mass storage from personal computers to portable entertainment devices. Like any other product of the electronics industry, hard drives are subjected to the inexorable law of miniaturization. Today, the main challenge of the hard disk manufacturers is to design a compact, fast, high storage devices at low cost.

In modern hard disk drives, multiple heads are used for fast recoding of data to the magnetic disk and retrieving of data from it. Since magnetic recording tracks have become narrower to increase in the areal density, the read-back signals of the tracks inevitably interfere with each other causing inter-track interference. Hence, a magnetic recording track can be modelled as a partial response channel that allows to interfere only with adjacent tracks and this type of interference is called the inter-track interference (ITI) [15]. When there exist an inter-track interference, single track decoding is not the optimal way of decoding the information in a magnetic recording media.

In this dissertation, we propose a new technique to design inner shaping codes for magnetic recording channel. We mainly focus on the low-rate code design schemes. For this, we assume that the magnetic recording channel is a frequency selective channel and try to design the optimum shaping codes by assuming that the shaping codes are the spreading sequences in an equivalent multiuser frequency selective system. It is important to note that the inputs to the magnetic recording channels are derived from a binary alphabet. Hence, we design the spreading sequences with binary chips. We will show in Chapter VI that our proposed algorithm in Chapter IV to design finite alphabet spreading sequences for frequency selective channel can successfully be used to design above shaping sequences for magnetic recording channels.

The rest of the dissertation is organized as follows. The second chapter gives the necessary background for the discussions of the dissertation work coming in following chapters. Third chapter introduces the spectral domain approach to design

the spreading sequences for frequency selective channels. In Chapter IV, we discuss the design of constrained alphabet and amplitude sequences based on the spectral properties of unconstrained spreading sequences. Chapter V discusses the design of constrained alphabet sequences based on the water-filling algorithm. In Chapter VI, the design of shaping codes for single-head and multi-head magnetic recoding channels is discussed. Finally, Chapter VII gives the conclusion of the dissertation.

CHAPTER II

BACKGROUND

In this chapter, we provide the necessary theoretical background that is required in the later chapters of this dissertation. First, we discuss the system model for a multiuser DS-CDMA system. Then, we discuss different types of optimum and suboptimum receivers for a DS-CDMA system which are used to separate the users' information in a multiuser environment. We also discuss the concept behind the turbo encoding and decoding schemes which is required in Chapter V. Finally we discuss about the low density parity check codes and EXIT charts which are useful in Chapter VI.

A. System model

Consider an uplink DS-CDMA system with K active users. Here, at the m th epoch, k th user's information symbol $x_{m,k}$ is spread using the user specific spreading sequence $s_k(t)$, modulated by a carrier frequency f_c and transmitted over the channel $h_k(t)$. The signal at the receiver's end is a linear combination of all the users received signal and it is corrupted by additive white Gaussian noise $n(t)$ with double-sided spectral density $N_0/2$. The received signal $r(t)$ can be represented as

$$r(t) = \sum_k^{K-1} \sum_m x_{k,m} h_k(t - mT) s_k(t - mT) \cos(2\pi f_c t + \theta) + n(t) \quad (2.1)$$

where $h_k(t) = \sum_{j=0}^{L-1} h_{k,j} \delta(t - jT_c)$ and $s_k(t) = \sum_{j=0}^{N-1} s_{k,j} P(t - jT_c)$ while $P(t)$ is the shaping pulse. T is the symbol duration.

The received signal is converted to a baseband signal by down-converting with the use of a locally generated oscillator matched to the carrier frequency f_c with phase offset θ . Then, the demodulated signal is passed through a chip-matched filter $P^*(t)$. Assuming $L \ll N$, that is ignoring the inter-symbol interference (inter-chip

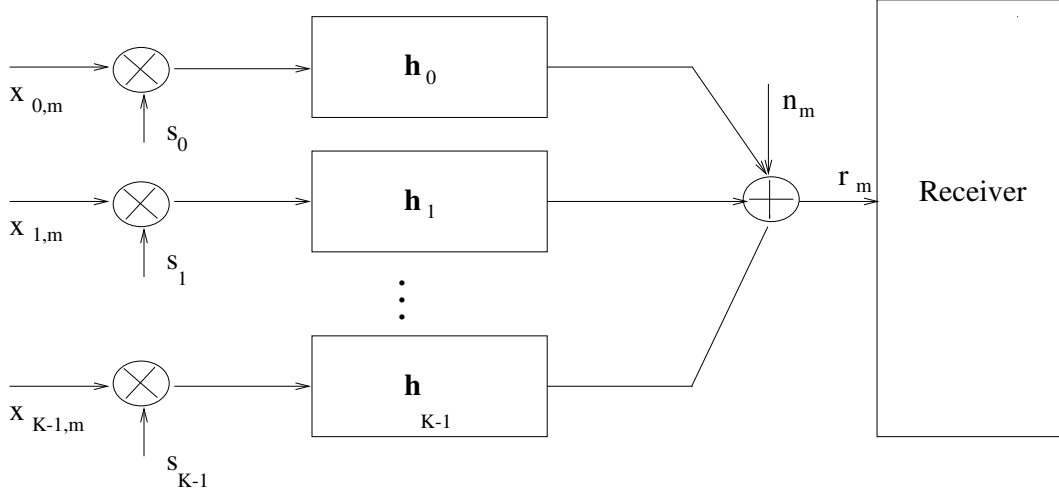


Fig. 1. Block diagram of a synchronous uplink DS-CDMA system.

interference still exists), the output of the chip level matched filter at the base station for the q th chip interval is given by

$$r_{q,m} = \sum_{k=0}^{K-1} \sum_{j=0}^{L-1} x_{k,m} s_{k,q-j} h_{k,j} + n_{q,m}, \quad 0 \leq q \leq N-1 \quad (2.2)$$

where $r_{q,m} = \int_{mT}^{mT+qT_c} r(t) p^*(t - (mT + qT_c)) dt$ and $n_{q,m} = \int_{mT}^{mT+qT_c} n(t) p^*(t - (mT + qT_c)) dt$. The channel between the k th user's transmitter and the receiver (base station) is assumed to be a frequency selective slow fading channel. Here, $\mathbf{s}_k = [s_{k,0}, s_{k,1}, \dots, s_{k,N-1}]^T$ is the spreading sequence of length N for the k th user. The k th user's channel with L taps is given by the vector $\mathbf{h}_k = [h_{k,0}, h_{k,1}, \dots, h_{k,L-1}]^T$. This discrete time model simplifies most of our theoretical analysis and simulations and the corresponding block diagram of a K user synchronous uplink DS-CDMA system is shown in Fig. 1.

Equation (2.2) can be written in vector form as

$$\mathbf{r}_m = \sum_k^K \mathbf{H}_k \mathbf{s}_k x_{k,m} + \mathbf{n}_m \quad (2.3)$$

where $\mathbf{n}_m = [n_{0,m}, n_{1,m}, \dots, n_{N-1,m}]^T$, $\mathbf{r}_m = [r_{0,m}, r_{1,m}, \dots, r_{N-1,m}]^T$ and \mathbf{H}_k is an $N \times N$ matrix given by

$$\mathbf{H}_k = \begin{bmatrix} h_{k,0} & 0 & 0 & \dots & 0 \\ h_{k,1} & h_{k,0} & 0 & \dots & 0 \\ \vdots & h_{k,1} & h_{k,0} & \dots & \vdots \\ h_{k,L-1} & \vdots & h_{k,1} & \dots & \vdots \\ \vdots & \vdots & \vdots & \dots & h_{k,0} \end{bmatrix}.$$

Here, the first column of \mathbf{H}_k is \mathbf{h}_k followed by $N - L$ zeros. The rest of the columns are obtained by downshifting the first column of \mathbf{H}_k . Further, if the k th user's filtered spreading sequence is \mathbf{f}_k which is given by $\mathbf{f}_k = \mathbf{H}_k \mathbf{s}_k$, then, \mathbf{r}_m can be represented as

$$\mathbf{r}_m = \sum_k^K \mathbf{f}_k x_{k,m} + \mathbf{n}_m. \quad (2.4)$$

B. Multiuser detectors in a DS-CDMA system

In a downlink DS-CDMA system, each mobile communication unit concerns only on the detection of its own signal while in the uplink, the base station detects all active users' signals simultaneously or separately. The optimal detector for the joint detection of the users' information is the maximum likelihood (ML) detector which simultaneously detects all the users's information symbols. Unfortunately the computational complexity of the maximum likelihood detector increases exponentially with the number of users, hence it has a very little practical significance. In literature, several suboptimal detectors have been proposed for DS-CDMA systems which will be briefly discussed in this subsection [16].

In conventional matched filter detection method, k th user's receiver is simply a

matched filter given by \mathbf{f}_k . Hence, the k th user's decoded signal is given by

$$\hat{\mathbf{x}}_{k,m} = |\mathbf{f}_k|^2 \mathbf{x}_{k,m} + \sum_{j \neq k}^K \mathbf{f}_k^H \mathbf{f}_j \mathbf{x}_{j,m} + \mathbf{f}_k^H \mathbf{n}_m \quad (2.5)$$

It can be clearly seen from the expression that, depending on the cross correlations among the filtered sequences, the k user's bit error rate (BER)/SINR performance varies. Hence, with the use of a matched filter, much care has to be taken to design sequences such that the cross correlations among the filtered spreading sequences are significantly small.

1. De-correlator detector

Using the previous section's results, the output vector of bank of K matched filters can be written as

$$\mathbf{z}_m = \mathbf{F}^H \mathbf{F} \mathbf{x}_m + \hat{\mathbf{n}}_m \quad (2.6)$$

where \mathbf{F} is an $N \times K$ matrix with the k th column \mathbf{f}_k and $\hat{\mathbf{n}}_m = \mathbf{f}_k^H \mathbf{n}_m$. Let the cross correlation matrix of the filtered sequences $\mathbf{R} = \mathbf{F}^H \mathbf{F}$ be invertible. Then we can pre-multiply the received vector by \mathbf{R}^{-1} resulting

$$\hat{\mathbf{x}}_m = \mathbf{x}_m + \mathbf{R}^{-1} \hat{\mathbf{n}}_m \quad (2.7)$$

It can be seen that the de-correlator detector completely removes the multiple access interference but, this could lead to a noise enhancement.

2. MMSE detector

To achieve a certain tradeoff between interference rejection and noise enhancement, linear MMSE detectors are used in CDMA systems. The goal here is to find a linear detector \mathbf{c}_k for each user k such that $E[|x_{k,m} - \langle \mathbf{c}_k, \mathbf{z}_m \rangle|^2]$ is minimized. The cor-

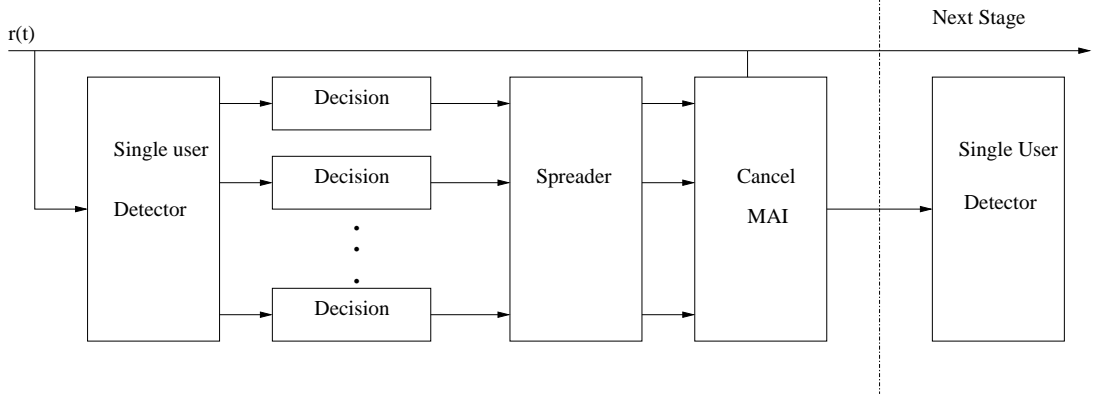


Fig. 2. Block diagram of a multiuser detector.

responding \mathbf{c}_k is given by $[\mathbf{R} + \sigma^2 \mathbf{I}]^{-1} \mathbf{H}_k \mathbf{s}_k$. Here, σ^2 is the noise variance. When $\sigma \rightarrow \infty$, \mathbf{c}_k becomes the matched filter detector while when $\sigma \rightarrow 0$, \mathbf{c}_k becomes the de-correlator detector.

3. Successive interference cancellation

The performances of the suboptimal detectors as the matched filter detector, the de-correlator detector and the linear MMSE detector are inferior to the maximum likelihood detector when the cross correlations among the sequences are significant. However, the use of maximum likelihood detector is prohibitively complex. To circumvent this problem, a new form of joint detection scheme is proposed in the literature. These decoders are generally called as multistage detectors. There are two types of multistage detectors: parallel interference cancellers and serial interference cancellers. Let's assume the output signal at the k th user's matched filter is as

$$z_{k,m} = \sum_{j=0}^{N-1} f_{k,j}^* r_{j,m}, \quad 0 \leq k \leq K-1. \quad (2.8)$$

Fig. 2 shows a block diagram of a parallel interference cancellation based mul-

tiuser detector. The following iterative steps briefly describe the function of the parallel interference cancellation based multiuser detector [17].

1. Estimate the k th user's bit by $\hat{x}_{k,m} = \text{sgn}(z_{k,m})$.
2. Reconstruct the multiple access interference for each user k based on the estimation obtained in step 1. Let us assume that the calculated interference for the n th iteration for the k th user is $I_{k,n}$.
3. For each user k , subtract multiple access interference (MAI) given by $I_{k,n}$ from the received signal \mathbf{r}_m . Here $I_{k,0} = 0$. This interference reduced signal can be considered as the new input to the k th user's matched filter to get a more accurate decision for the k th user's bit, $x_{k,m}$.
4. Steps 2 and 3 are followed iteratively for a sufficient number of times until the BER of each user converges.

An improved version of the parallel interference canceller is introduced in [18] where, for each user, the weighted multiple access interference (WMAI) given by $(w_1 I_{k,n} + w_2 I_{k,n-1}) / (w_1 + w_2)$ is subtracted. The parallel interference cancellation scheme works very well when there is no or less near-far ratio effect.

In serial or successive interference cancellation schemes, the user with the highest received power is detected first. Once that user is detected, the user's signal is reconstructed and subtracted from the received signal. Then, the user with the second highest received power is detected. Similarly the rest of the users are detected according to the descending order of their received powers.

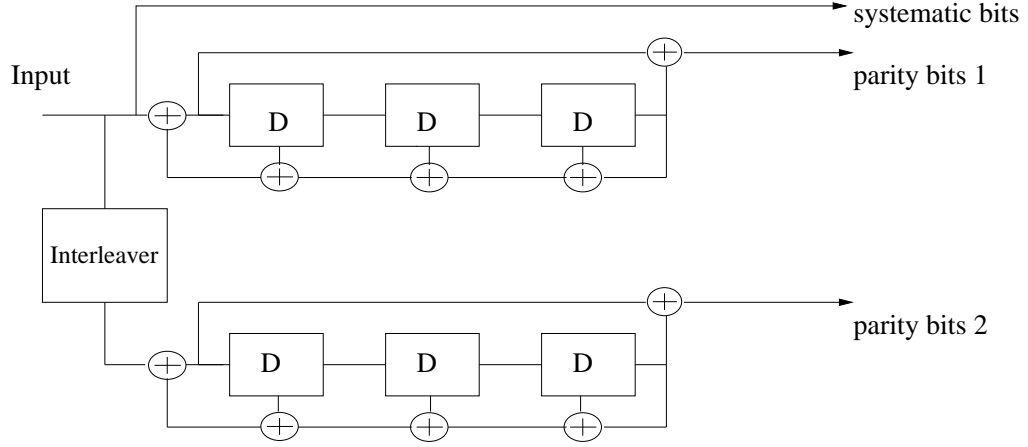


Fig. 3. Block diagram of a turbo encoder.

4. Turbo codes

In their landmark paper [19], Berrou, Glavieux and Thitimajshima proposed a new coding scheme that performs very close to the Shannon capacity. These codes were later baptized as turbo codes. The main idea of turbo codes is to use two recursive systematic convolution codes with an interleaver in between. Fig. 3 gives the basic block diagram of a turbo encoder. At the output of the encoder, parity bits are punctured to get the required information rate.

A turbo code can be regarded as a large block code and its performance depends not only on the minimum distance of constituent codes but also on the overall weight distribution of the constituent codes [20]. The role of the interleaver is to make the input patterns giving low weight codewords to be interleaved to produce high weight codewords.

The optimum decoding scheme for turbo codes is a maximum likelihood decoder. However, the interleaver embedded in the encoder structure causes the joint trellis to have extremely large number of states and practical implementation of ML detection

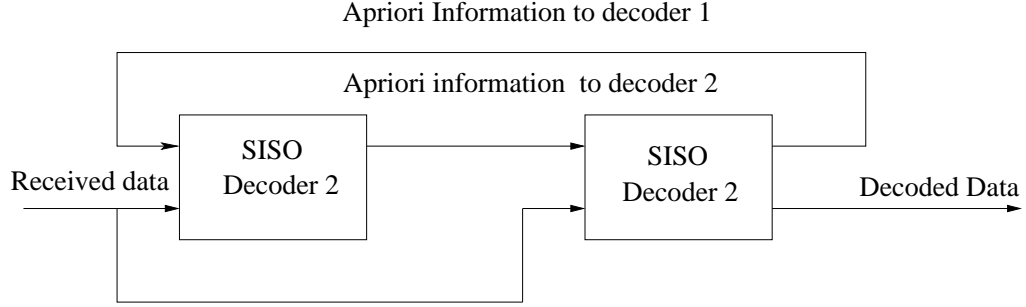


Fig. 4. Block diagram of a turbo decoder.

of turbo codes is nearly impossible. To overcome this obstacle, a suboptimal iterative decoding scheme is proposed.

Fig. 4 shows a basic block diagram of a turbo decoder. Each constituent Soft input soft output (SISO) decoder obtains two types of soft inputs. They are, *apriori* information and systematic information that is provided by systematic bits. At the first stage, there will be no *apriori* information for the SISO decoder 1. Then the decoder exploits the Markov structure of the coded bits to the first encoder and produces the soft outputs which measure the reliability of the information bits. The output information consists of three types of information. They are the *apriori* and systematic information provided at the input of the encoder and the extrinsic information exploited by the decoder using the Markov structure of the coded bits. SISO decoding algorithms follows the BCJR decoding algorithm proposed in [21]. The extrinsic information is interleaved and fed back to the SISO decoder 2 which will consider this information as the *apriori* information for the second decoder. From SISO decoder 2, new extrinsic information is generated and the interleaved version of the information is fed back to the first decoder and so on.

5. Low density parity check codes

Low density parity check codes are a class of linear block codes and were first introduced in [22] by Gallager in 1960 and reinvented by MacKay in 1999 [23]. The name low density parity check (LDPC) codes comes from the characteristics of the parity check matrix of the code which contains only few non-zero entries. There are two types of LDPC codes called regular LDPC codes and irregular LDPC codes. For regular LDPC codes, the weight of the every column and row in the parity check matrix is the same. For irregular LDPC codes, the number of ones in rows and columns are not the same. LDPC codes perform very close to the channel capacity for a variety of channels. In [24], Tanner introduced a graphical representation for LDPC codes

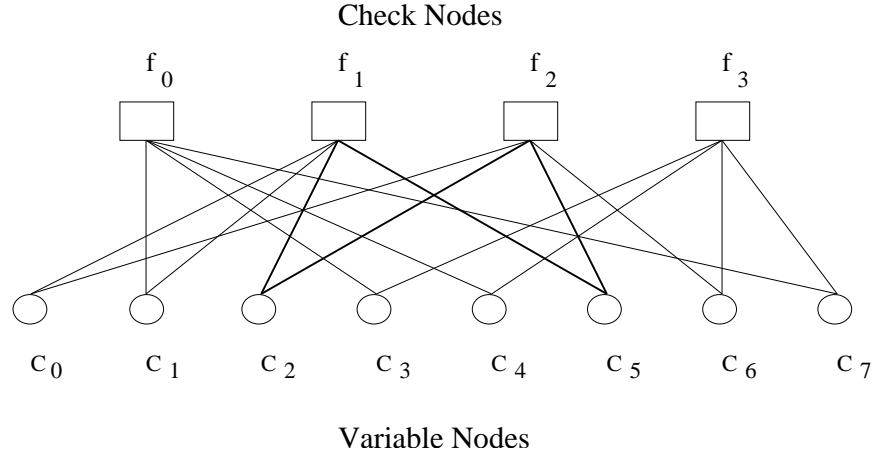


Fig. 5. Graph structure of an LDPC code.

which not only provides the complete description of codes but also helps to describe the decoding algorithm for these codes. Tanner graph is a bipartite graph where the nodes of the graph are separated into two sets of nodes called the variable nodes and the check nodes. The number of variable nodes corresponds to the number of symbols in the codeword and the number of check nodes corresponds to the number of parity

bits. The edges of the Tanner graph are arranged such that the code bits satisfy the parity checks in the code. Fig. 5 shows the Tanner graph for a (7,4) hamming code.

The most commonly used decoding algorithm for LDPC codes is the message passing algorithm [25],[26]. In this algorithm, in each half iteration, a variable node processes its input message and passes it to the neighboring check node (Neighboring nodes are the nodes that are connected by an edge). In the next half of the iteration, each check node processes its input messages passed from the neighboring check nodes and passes its resulting extrinsic information back to the neighboring check nodes. This iterative process is carried out until it achieves some stopping criteria and finally, the decoder performs a decision on the coded bits.

6. Extrinsic information transfer chart

The extrinsic information transfer (EXIT) chart pioneered by ten Brink [27] is a powerful technique which is used to analyze the convergence behavior of iterative decoding techniques. As we have discussed earlier, in the turbo decoding technique, each constituent decoder obtains apriori and systematic information and produces extrinsic information which is considered as the apriori information for the second decoder. In the iterative decoding scheme that discussed earlier, information transfer between the two decoders is not easy to analyze and to describe. In [27], ten Brink proposed that by studying how the extrinsic information evolves in a constituent decoder with respect to apriori information, it is possible to analyze the convergence behavior of iterative decoders. Specifically, if X represents systematic information, EXIT chart is the plot of $I(L_e; X)$ versus $I(L_a; X)$ or the plot $I(L_e; X) = T(I(L_a; X))$. Where, $I(L_e; X)$ is the mutual information between X and extrinsic information L_e and $I(L_a; X)$ is the mutual information between X and apriori information L_a . It is proved that for a binary erasure channel, the area under the EXIT chart corresponds

to the channel code-rate under optimal decoding [28].

In Chapter VI, we design inner shaping codes for frequency selective channels such that the EXIT chart for the inner code is almost flat. In this scenario, the outer code observes a channel which is equivalent to an AWGN channel. Hence, the outer codes matched to an AWGN channel will also be optimum for the frequency selective channels with our designed inner shaping codes and this simplifies the design of the outer code for those channels.

CHAPTER III

A SPECTRAL DOMAIN APPROACH TO DESIGN SPREADING SEQUENCES FOR FREQUENCY SELECTIVE FADING CHANNELS

In this chapter, we propose a new way of designing spreading sequences by analyzing their frequency domain characteristics. We show that for frequency selective channels, designing of spreading sequences subjected to maximizing SINR is similar to designing spreading sequences by concentrating their spectra at the spectral peaks of the channels' responses while avoiding the overlapping of spectra of the sequences if possible. We will further show that it is possible to represent each user's spreading sequence with fewer parameters in the frequency domain than that of in the time domain. This allows the reduction in the computational complexity and the feedback bandwidth required and improves the performance of some existing algorithms.

A. Background

First, we will briefly look into the joint transmitter receiver adaptation scheme proposed by Rajappan and Honig [9] as this will facilitate an understanding of the techniques proposed here. Here, we consider a group optimization of signature sequences where in the optimization, each user's SINR is iteratively maximized assuming other users' signals as interference. Further, we assume that the design is performed at the base station and the perfect channel state information is available both at the transmitter and at the receiver.

For this analysis, we assume the discrete time model proposed in the section A of Chapter II, which is given by

$$\mathbf{r}_m = \sum_k^K \mathbf{H}_k \mathbf{s}_k x_{k,m} + \mathbf{n}_m. \quad (3.1)$$

Then, the output of the k th user's receiver filter corresponding to the m th bit is given by

$$y_{k,m} = \mathbf{c}_k^H \mathbf{r}_m. \quad (3.2)$$

Let the k th user's receiver be a matched filter given by

$$\mathbf{c}_k = \frac{\mathbf{H}_k \mathbf{s}_k}{\|\mathbf{H}_k \mathbf{s}_k\|} \quad (3.3)$$

and let the SINR output of the user's matched filter be given by

$$\gamma_k = \frac{|\mathbf{c}_k^H \mathbf{H}_k \mathbf{s}_k|^2}{\mathbf{c}_k^H \mathbf{R}_k \mathbf{c}_k} \quad (3.4)$$

where $\mathbf{R}_k = \sum_{p=0, p \neq k}^{K-1} \mathbf{H}_p \mathbf{s}_p \mathbf{s}_p^H \mathbf{H}_p^H + \sigma^2 \mathbf{I}$ is the interference plus noise covariance matrix.

As shown in [9], the k th user's spreading sequence \mathbf{s}_k that maximizes the user's SINR under constrained transmitter power p , is the solution to the maximization problem

$$J_k = \gamma_k + \lambda(\mathbf{s}_k^H \mathbf{s}_k - p). \quad (3.5)$$

The optimum \mathbf{s}_k can be obtained by finding the solution for \mathbf{s}_k satisfying

$$\mathbf{H}_k^H \left[2\mathbf{I} - \frac{\mathbf{s}_k^H \mathbf{H}_k^H \mathbf{H}_k \mathbf{s}_k \mathbf{R}_k}{\mathbf{s}_k^H \mathbf{H}_k^H \mathbf{R}_k \mathbf{H}_k \mathbf{s}_k} \right] \mathbf{H}_k \mathbf{s}_k = \mathbf{s}_k^H \mathbf{H}_k^H \mathbf{H}_k \mathbf{s}_k \mathbf{s}_k. \quad (3.6)$$

It can be clearly seen from (3.6) that the k th user's spreading sequence is the eigenvector of the matrix $\mathbf{H}_k^H \left[2\mathbf{I} - \frac{\mathbf{s}_k^H \mathbf{H}_k^H \mathbf{H}_k \mathbf{s}_k \mathbf{R}_k}{\mathbf{s}_k^H \mathbf{H}_k^H \mathbf{R}_k \mathbf{H}_k \mathbf{s}_k} \right] \mathbf{H}_k$ that maximizes (3.5). The optimum set of spreading sequences that maximizes $\sum_{k=0}^{K-1} \gamma_k$ can be obtained using coordinate ascent method [29]. That is, at each iteration, we fix all but the k th user's spreading sequence \mathbf{s}_k and optimize \mathbf{s}_k . Iterations are performed over all the users until the global maximum is obtained. In the above algorithm, spreading sequences are initialized with a properly normalized random vector of length N and the final value for

the k th user's spreading sequence can be found by calculating \mathbf{s}_k in (3.6) iteratively until it converges [9].

B. Frequency domain characteristics of good spreading sequences

Here, we consider a single user DS-CDMA system in a frequency selective environment. Now, if we consider the single user optimization with a matched filter receiver, the optimum spreading sequence is the solution to

$$J = \mathbf{s}_k^H \mathbf{H}_k^H \mathbf{H}_k \mathbf{s}_k + \lambda(\mathbf{s}_k^H \mathbf{s}_k - p). \quad (3.7)$$

The solution to the above optimization problem is given by

$$\mathbf{H}_k^H \mathbf{H}_k \mathbf{s}_k = \left[\mathbf{s}_k^H \mathbf{H}_k^H \mathbf{H}_k \mathbf{s}_k \right] \mathbf{s}_k. \quad (3.8)$$

Since $\mathbf{H}_k^H \mathbf{H}_k$ is a Hermitian matrix, we can perform the singular value decomposition of the matrix $\mathbf{H}_k^H \mathbf{H}_k$ as [30]

$$\mathbf{H}_k^H \mathbf{H}_k = \mathbf{U}_k^H \mathbf{\Lambda} \mathbf{U}_k. \quad (3.9)$$

Further, we can observe that \mathbf{H}_k is a Toeplitz matrix. Using the asymptotic ($N \gg 1$) equivalence of a Toeplitz and a circulant matrix [31], we can conclude that the eigenvalues of \mathbf{H}_k are the DFT coefficients of \mathbf{h}_k and \mathbf{U}_k is the DFT transform matrix. Hence, by simplifying, (3.8) can be expressed as

$$\mathbf{\Lambda} \mathbf{f}_k = \chi \mathbf{f}_k \quad (3.10)$$

with $\chi = \mathbf{s}_k^H \mathbf{H}_k^H \mathbf{H}_k \mathbf{s}_k$ and \mathbf{f}_k is the DFT of the k th user's spreading sequence \mathbf{s}_k .

It can be clearly seen that the optimum spreading sequence is the eigenvector corresponding to the maximum eigenvalue of $\mathbf{H}_k^H \mathbf{H}_k$. That is, the optimum spreading sequence for a single user system is a sequence whose spectrum is an impulse at the

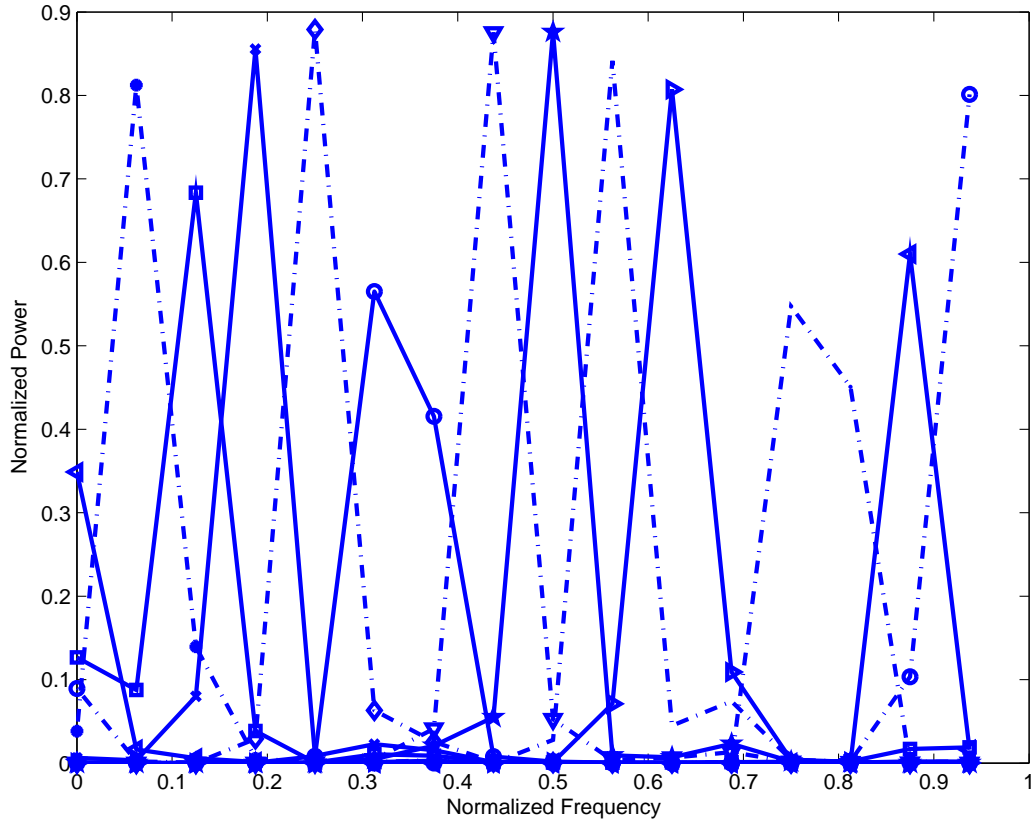


Fig. 6. Power spectrum of each user's spreading sequence.

frequency where the channel frequency response has the highest magnitude. However, for a multiuser CDMA system, it is not enough just to maximize the individual user's performance since each user's performance depends on the interference induced by the other users. Hence, the objective must be to maximize each user's performance while keeping the cross correlation among the users' spreading sequences at a sufficiently low value. According to Parseval's theorem, the cross correlation between two sequences in the frequency domain is the same as that of in the time domain. That is, we can design the sequences in the frequency domain instead of designing them in the time domain considering the criteria for minimizing the interference among the users

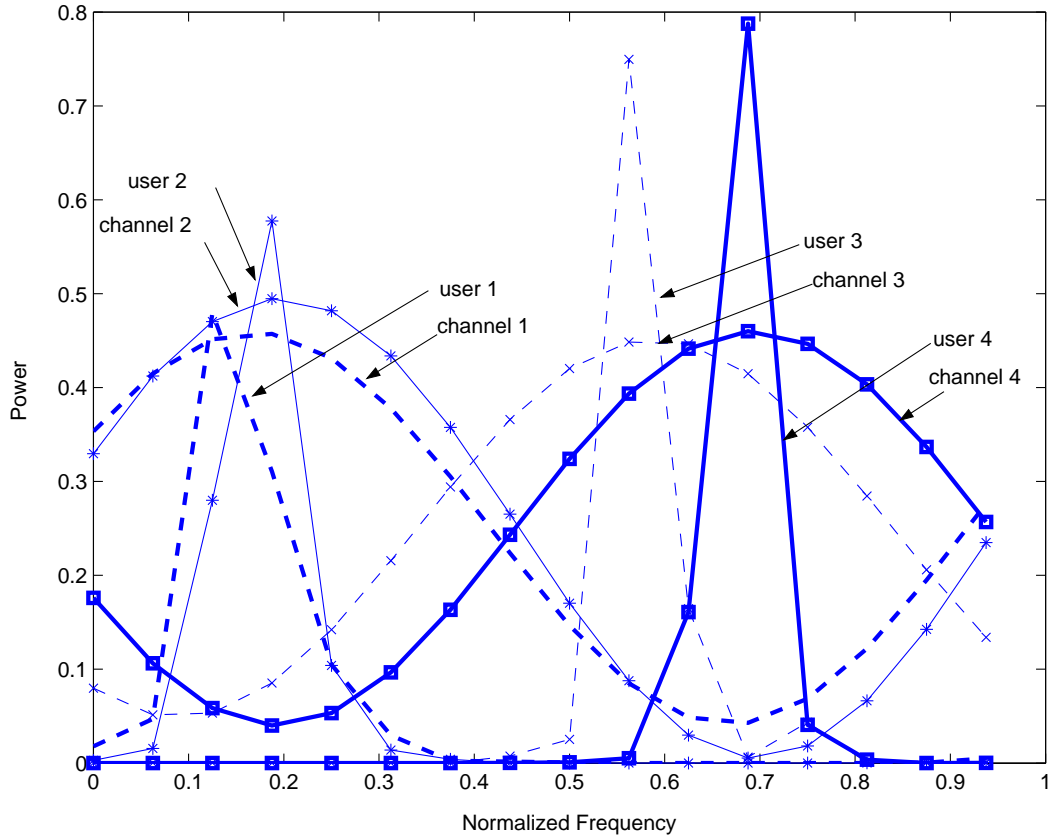


Fig. 7. Power spectrum of each user's spreading sequence. Only four of the users' sequences' spectra and channels' spectra are shown.

as the minimization of the frequency domain cross correlation among the users. It is worthwhile to study the characteristics of well-designed spreading sequences for multipath channels in the frequency domain.

To observe how the optimized spreading sequences are positioned in the frequency domain in a multiuser environment, we have computed the optimum set of spreading sequences using the iterative algorithm in (3.6) for a 12 user system. The spreading length used is 16. Each user's channel is assumed to be a randomly generated two path channel and kept fixed throughout the simulation.

As seen in Fig. 6 and Fig. 7, the frequency spectrum of each user's spreading sequence is narrow band and lies around the frequencies of that user's strongest channel components (To preserve clarity of the figure, only 4 of the 16 users' spectra are included). Further, the figure illustrates that for users whose strongest channel components occur at different frequencies, the spectra of the optimum spreading sequences have little or no overlap. It was also verified that when two or more users' channels have the same frequency as the strongest channel component, although the spectra of those user's spreading sequences overlap, correlations among those sequences are small. For example, in Fig. 7, user 1 and user 2 have overlapping spectra. In this case, the adaptation algorithm in (3.6) adapts amplitudes and phases of those 2 users' spreading sequences such that the cross correlation between those 2 users' spreading sequences is minimized (The normalized cross correlation in this case was 1.173×10^{-4}).

While the above example shows the typical spectra of the spreading sequences, it is only one example. It is quite difficult to analytically prove this behavior. In order to make a more convincing argument about the spectra of the spreading sequences and their relation to the frequency response of the channel, we consider the cumulative distribution function (CDF) of the amount of power contained in the D strongest frequency components of the optimized spreading sequence. In order to explain this further, let the k th user's spreading sequence, optimized by the adaptive algorithm in [9] be \mathbf{s}_k and the filtered version of \mathbf{s}_k after passing through the channel \mathbf{h}_k be given by $\mathbf{w}_k = \mathbf{h}_k \odot \mathbf{s}_k$, where \odot refers to the convolution operation. Let the N -point discrete Fourier transforms of the sequences \mathbf{s}_k and \mathbf{w}_k be given by $[\mathbf{s}_k(\lambda_0), \mathbf{s}_k(\lambda_1), \dots, \mathbf{s}_k(\lambda_{N-1})]^T$ and $[\mathbf{w}_k(\lambda_0), \mathbf{w}_k(\lambda_1), \dots, \mathbf{w}_k(\lambda_{N-1})]^T$ respectively. If $\mathbf{l}_k = \{l_1, l_2, \dots, l_D\}$ are the k th user's channel's strongest D frequency components in decreasing order of magnitude of the spectrum, then we define power

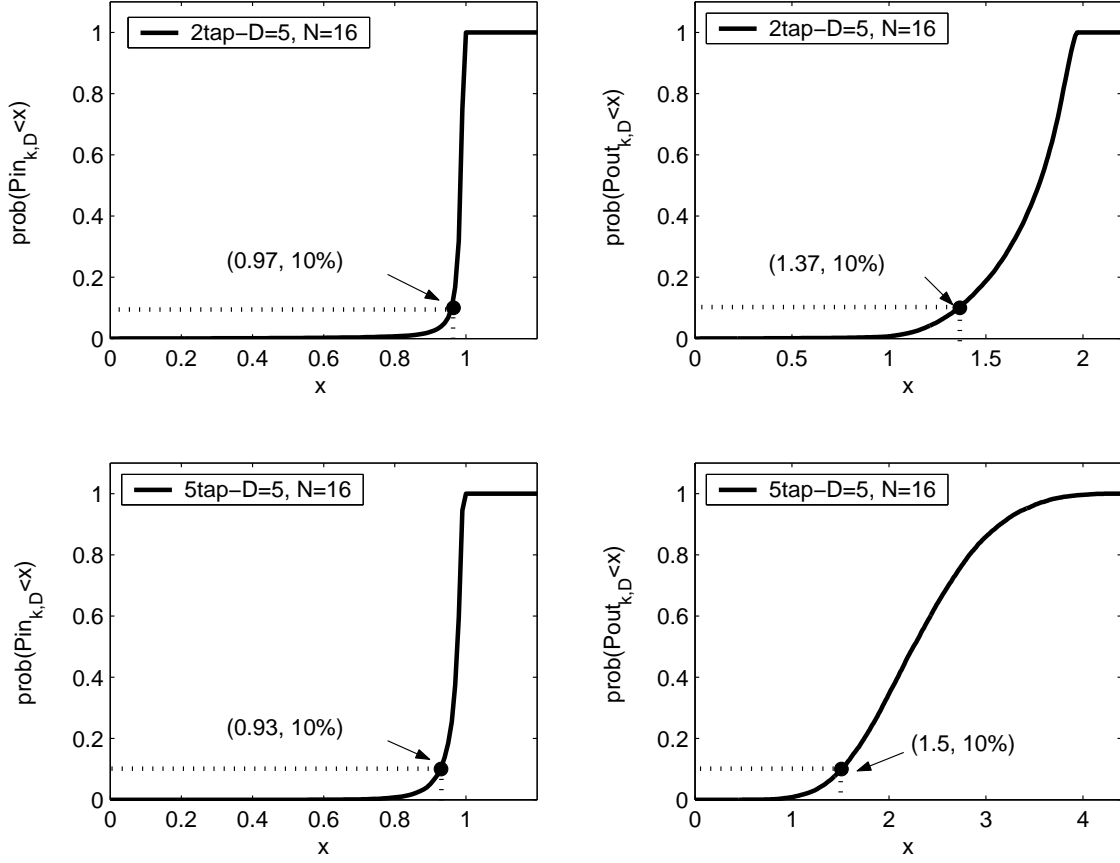


Fig. 8. Cumulative Density Functions (CDFs) of the transmitted and the received power of users' spreading sequences.

of \mathbf{s}_k and \mathbf{w}_k confined to D frequency components as $Pin_{k,D} = \sum_{\forall r \in I} |\mathbf{s}_k(\lambda_r)|^2$ and $Pout_{k,D} = \sum_{\forall r \in I} |\mathbf{w}_k(\lambda_r)|^2$.

Fig. 8 shows the CDF's of $Pin_{k,D}$ and $Pout_{k,D}$ for $D = 5$. Both 2-tap and 5-tap channels are considered and the CDFs are obtained over 10^5 channel realizations. The power of \mathbf{s}_k is normalized to 1. It can be observed from the figure that 90% of the time, most of the power of the optimized spreading sequence \mathbf{s}_k (97% and 93% of the power of \mathbf{s}_k in 2-tap and 5-tap channels, respectively) is confined to a much narrower band than the available bandwidth. Further, we can see from the CDFs for

the power in the filtered sequences (received power) that, 5-tap channels provide much higher output power ($P_{out_{k,D}}$) than that of 2-tap channels. This is because that 5-tap channels provide more frequency selectivity than 2-tap channels resulting spectral peaks with much higher gains. Since the bandwidth of the optimized sequences are bandlimited and localized around those peaks, the transmitted power of the sequences are amplified by the spectral peaks, hence, providing much higher output power than that of in 2-tap case. If the frequency spectrum of an optimized spreading sequence were flat, there would not be a such power gain at the output of the channel. From these observations we draw some important conclusions.

1. Since most of the power in the optimized spreading sequences is concentrated in a few frequency components, it is possible to represent each user's spreading sequence with less number of parameters. Since the transmitter (e.g. mobile unit) has to obtain the information about the user's spreading sequence from the receiver (e.g. base station) through the reverse channel, this representation of sequences with less number of parameters allows the reduction of data overhead in the feedback channel. With a small abuse of terminology, we will refer to spreading sequences as being narrowband if most of the power is concentrated in a few (not necessarily contiguous) strongest frequency components.
2. There are some existing algorithms to design spreading sequences for multipath channels with low cross correlations. But, some of those algorithms attempt to optimize received power (received power normalized by the channel gain) and do not guarantee that the designed sequences will successfully exploit the channel gain. By observing each user's channel response, we can impose an additional constraint on the sequences so that the received absolute power will be high. We will show that by doing so, we can optimize the transmitter power

and improve the system performance of some already existing algorithms (e.g. [10]).

3. It is possible to simplify the existing sequence design algorithms. This is because, since the bandwidth of the spreading sequences are narrow, the users can be grouped into different frequency regions. Hence, the optimization can be done separately for separate groups with less complexity. This technique will be used to design the spreading sequences with constrained amplitudes and phases.

The applications of each of the above conclusions will be discussed in following sections.

C. Designing of spreading sequences with unconstrained amplitudes and phases in the frequency domain

In this section, we discuss some applications for the design of suitable spreading sequences with unconstrained amplitudes and phases for multipath channels, where we can make use of the important conclusions reached in the previous section. In subsections 2 and 3 of this chapter, we propose to improve the performance of some existing sequence design algorithms for multipath channels by implementing them in the frequency domain rather than in the time domain.

1. Main idea

Since the length of each user's spreading sequence is N , it is possible to represent each user's spreading sequence with N linearly independent basis vectors. For example, the set of N linearly independent basis vectors can be selected as $\{\mathbf{f}_0, \mathbf{f}_1, \dots, \mathbf{f}_{N-1}\}$,

where \mathbf{f}_r is given by

$$\mathbf{f}_r = \left[1, e^{\frac{j2\pi r}{N}}, e^{\frac{j2\pi 2r}{N}}, \dots, e^{\frac{j2\pi(N-1)r}{N}} \right], \quad 0 \leq r \leq N-1. \quad (3.11)$$

It is clear that, \mathbf{f}_r corresponds to a sinusoid (or rows of the DFT transform matrix) whose frequency response is an impulse at the r th frequency index and the k th user's spreading sequence can be represented by

$$\mathbf{s}_k = \sum_{r=0}^{N-1} a_{k,r} \mathbf{f}_r. \quad (3.12)$$

According to the analysis in section B, the optimized spreading sequences are narrow band. Hence, it is possible to represent each user's spreading sequence with fewer parameters with significant accuracy. For this, we select each user's spreading sequence as a linear combination of a set of basis vectors considering that each user's basis is a set of sinusoids whose frequency components are located at the strongest frequency components of the corresponding user's channel. For example, if a user's channel's strongest D frequency components are located at $\mathbf{l} = \{l_1, l_2, \dots, l_D\}$ in decreasing order of magnitude of the spectrum, then the corresponding optimum spreading sequence is approximated by

$$\mathbf{s}_k = \sum_{\forall r \in \mathbf{l}} a_{k,r} \mathbf{f}_r. \quad (3.13)$$

This allows us to select the best smallest set of vectors as each user's basis.

2. Proposed modification to the approach in [32]

It can be seen that, for unconstrained amplitude spreading sequences, the data overhead in the feedback channel is QN bits per user, where Q is the precision in bits for quantization of the unconstrained chip amplitudes. To reduce the overhead in the feedback path, Rajappan and Honig [32] have also introduced a reduced-rank trans-

mitter adaptation scheme where the signature sequences are constrained to lower dimensional subspaces spanned by some orthogonal basis vectors.

For example, if \mathbf{F}_k is the $N \times D$ matrix whose D columns are the basis vectors of the k th user, the optimum spreading sequence \mathbf{s}_k is a linear combination of D columns of \mathbf{F}_k given by $\mathbf{s}_k = \mathbf{F}_k \mathbf{a}_k$. In [32], it is assumed that the basis vectors for \mathbf{F}_k are randomly selected D orthonormal vectors. The corresponding \mathbf{a}_k value, with a minimum mean squared error receiver $\mathbf{c}_k = \mathbf{R}_k^{-1} \mathbf{H}_k \mathbf{s}_k$ (MMSE receiver assuming perfect knowledge of SNR), is given by

$$(\mathbf{F}_k^H \mathbf{F}_k)^{-1} \mathbf{F}_k^H \mathbf{H}_k^H \mathbf{R}_k^{-1} \mathbf{H}_k \mathbf{F}_k \mathbf{a}_k = \nu \mathbf{a}_k \quad (3.14)$$

and with a matched filter receiver $\mathbf{c}_k = \frac{\mathbf{H}_k \mathbf{s}_k}{\|\mathbf{H}_k \mathbf{s}_k\|}$, it is given by

$$(\mathbf{F}_k^H \mathbf{F}_k)^{-1} \mathbf{F}_k^H \mathbf{H}_k^H \left(\frac{2\mathbf{I}}{\mathbf{a}_k^H \mathbf{F}_k^H \mathbf{H}_k^H \mathbf{H}_k \mathbf{F}_k \mathbf{a}_k} - \frac{\mathbf{R}_k}{\mathbf{a}_k^H \mathbf{F}_k^H \mathbf{H}_k^H \mathbf{R}_k \mathbf{H}_k \mathbf{F}_k \mathbf{a}_k} \right) \mathbf{H}_k \mathbf{F}_k \mathbf{a}_k = \nu \mathbf{a}_k. \quad (3.15)$$

Equations (3.14) and (3.15) can be derived by selecting $\mathbf{s}_k = \mathbf{F}_k \mathbf{a}_k$ in (3.5) and maximizing it over \mathbf{a}_k for matched filter and MMSE receivers. It is clear that \mathbf{a}_k corresponds to an eigenvector of the matrices given in (3.14) and (3.15). The appropriate eigenvector is selected by finding the eigenvector that maximizes the SINR, given by $\gamma_k = \frac{|\mathbf{c}_k^H \mathbf{H}_k \mathbf{s}_k|^2}{\mathbf{c}_k^H \mathbf{R}_k \mathbf{c}_k}$ at the receiver output. For the k th user, \mathbf{a}_k has to be iteratively calculated and once it is found, the optimum spreading sequence can be calculated by $\mathbf{s}_k = \mathbf{F}_k \mathbf{a}_k$. According to the discussion in the beginning of this section, we have shown that, each user's spreading sequence can be represented by the best D basis vectors which are carefully selected according to the user's channel response. Hence, the selection of the k th user's subspace \mathbf{F}_k , as a set of sinusoids which lie at the frequencies of the D strongest frequency components of the k th user's channel, allows

the maximization of the received power rather than selecting an arbitrary set of D orthogonal vectors. Hence, with the proposed selection criteria for basis vectors, the algorithm proposed in (3.14) and (3.15) will be shown an improved performance over the scheme proposed in [32].

To verify the performance of the proposed method, simulations were carried out for a DS-CDMA system. Each user's channel is assumed to be an L -tap frequency selective channel, where taps are drawn from a Gaussian distribution and the power is normalized to one. Slow fading similar to that in [5]-[9] is assumed. That is, we assume that each user's channel experiences a frequency selective block fading. The block duration is long enough so that users' channels can be assumed to be fixed within the period that all the users' spreading sequences are being updated. Spreading sequence length N and the number of users K are selected corresponding to a 75% loading. Performance of each system is evaluated by averaging the users' performance in the given system over a large number of channel realizations. For the reduced-rank optimization, we consider two schemes. The first is the scheme proposed by Rajappan and Honig [32], where for each user, a subspace with dimensionality D is generated randomly according to the method discussed in [32]. The second is our proposed scheme, where each user's basis vectors are selected such that those vectors are D sinusoids whose spectra are frequency impulses centered at the user's strongest channel components. In this case, simulations were carried out for both uplink and downlink scenarios.

From Fig. 9, it can be seen that for the uplink with 2-tap channels with a single user MMSE receiver, our proposed scheme with $K = 12$, $N = 16$ and $D = 5$ provides a 2 dB gain at a bit error rate of 10^{-3} over the scheme in [32]. Further, the performance difference between the proposed scheme and the full-rank optimization scheme is small. Also note that the performance is close to the performance of a single user

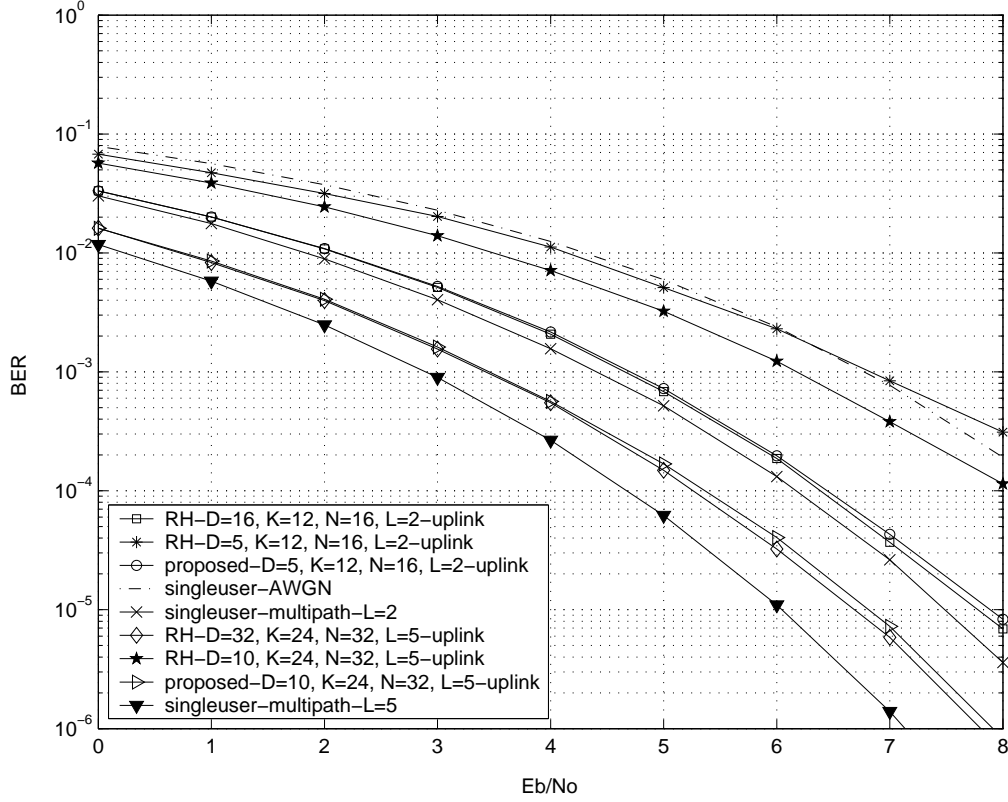


Fig. 9. Performance comparison of the two reduced-rank optimization schemes. RH=Rajappan and Honig algorithm [32].

when the ISI channel is perfectly known at the transmitter, which presents a lower bound on the achievable bit error rate.

To demonstrate the effect of the increase of channel taps on the system performance, we have simulated the proposed scheme with $L = 5$, $N = 32$ and $D = 10$ while keeping the overloading factor at 75% ($K = 24$). Fig. 9 shows that performances of all three schemes ([9],[32] and the proposed) are increased with the increase of the channel taps. This is expected since 5-tap channels provide more frequency selectivity. Further, we can see that our proposed scheme performs almost the same as the full-rank scheme. Proposed scheme outperforms the reduced-rank scheme in [32] by

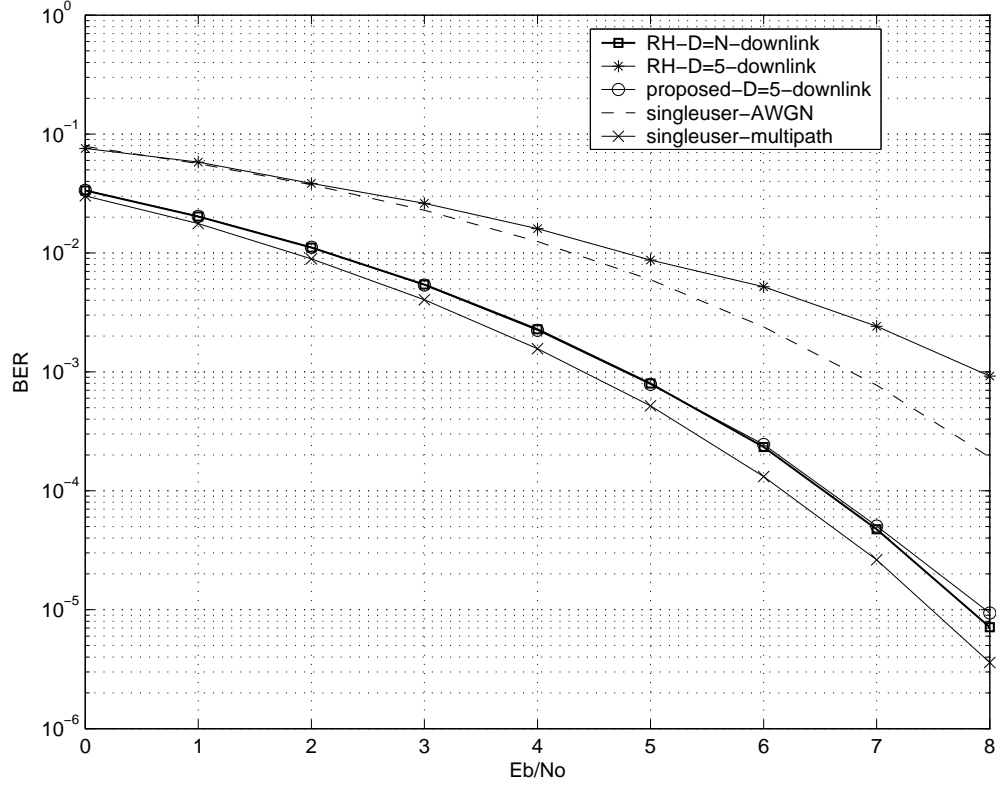


Fig. 10. Performance comparison of the two reduced-rank optimization schemes. RH=Rajappan and Honig algorithm [32]. $K=12$, $N=16$ and $L=2$.

about 2.5 dB. Fig. 10 shows that similar performance improvement can be obtained when the proposed scheme is used for the downlink. The results show that the proposed reduced-rank optimization provides similar performance to that of the full-rank optimization, but at a significantly reduced complexity and feedback bandwidth. In the overloaded case, the full-rank optimization scheme still tries to track the spectral peaks of the channel but, the algorithm cannot effectively minimize the cross correlation among overlapping users. This significantly high cross correlation cannot be handled by both the MMSE receiver and the matched filter receiver. For example, when $L = 2$, $N = 16$ and $K = 20$, an error floor around 10^{-2} was observed both in

full-rank adaptation and in the proposed scheme.

a. Computational complexity

We will compare the computational complexities of the full-rank optimization scheme and the proposed scheme with an MMSE receiver in (3.14) [33]. In the case of the full-rank optimization scheme, the expression (3.14) reduces to $\mathbf{H}_k^H \mathbf{R}_k^{-1} \mathbf{H}_k \mathbf{s}_k = \nu \mathbf{s}_k$ ($\mathbf{F}_k = \mathbf{I}_N$). The required number of computations to calculate \mathbf{R}_k and \mathbf{R}_k^{-1} are $N^2 K$ and $\frac{2}{3}N^3$ respectively [34]. Once \mathbf{R}_k^{-1} is calculated, we require $2(2L-1)N^2$ computations to calculate $\mathbf{H}_k^H \mathbf{R}_k^{-1} \mathbf{H}_k$. The eigenvectors can be calculated by $12N^3$ computations. Hence, the total number of computations required to calculate eigenvectors in (3.14) is $N^2 K + \frac{2}{3}N^3 + 2(2L-1)N^2 + 12N^3$. Once the eigenvectors are calculated, it is required to calculate the optimum eigenvector, that maximizes the SINR. For this, it can be shown that the required number of computations is $2N^3$. Hence, the total number of computations in each user iteration is $N^2 K + \frac{2}{3}N^3 + 2(2L-1)N^2 + 12N^3 + 2N^3$. For the proposed adaptation scheme, the matrix used to calculate the eigenvalues in the expression (3.14) can be rewritten as $(\mathbf{F}_k^H \mathbf{F}_k)^{-1} \mathbf{F}_k^H W^H W \mathbf{H}_k^H \mathbf{R}_k^{-1} \mathbf{H}_k W^H W \mathbf{F}_k$, where W is the Fourier transformation matrix. Since $(\mathbf{F}_k^H \mathbf{F}_k)$ is an identity matrix, no computation is required to calculate it. Similar to the full-rank scheme, we require $2(2L-1)N^2$ computations to calculate $\mathbf{H}_k^H \mathbf{R}_k^{-1} \mathbf{H}_k$. Both $\mathbf{F}_k^H W^H$ and $W \mathbf{F}_k$ can be calculated with $DN \log(N)$ computations. Further, $W \mathbf{F}_k$ is an $N \times D$ sparse matrix with only D non-zero entries all of which are 1, which will just permute the rows and columns of the matrix $\mathbf{H}_k^H \mathbf{R}_k^{-1} \mathbf{H}_k$. To calculate the DFT of $\mathbf{H}_k^H \mathbf{R}_k^{-1} \mathbf{H}_k$ twice we need $2N^2 \log(N)$ computations. Finally, to calculate the eigenvalues we require $12D^3$ computations. To find the optimum eigenvalue, another $2D^2 N + 2N^2 D$ computations are needed. Hence, the required number of total computations is $N^2 K + \frac{2}{3}N^3 + 2(2L-1)N^2 + DN \log(N) + 2N^2 \log(N) + 12D^3 + 2D^2 N + 2N^2 D$.

For $Q = 8$, $N = 16$ and $D = 5$, the required computation is only 23% of that for the full-rank case. For sufficiently large N , this fraction reduces to $\sim \frac{2/3N^3+N^2K}{2/3N^3+14N^3} = \frac{2+3K/N}{44} < 12\%$, which is a significant reduction.

b. Required feedback bandwidth

In the proposed scheme, to convey each user's optimized spreading sequence from the base station to the mobile unit, it is required to transmit QD bits plus the frequency indices of the D strongest channel components which requires $D \log_2(N)$ bits. Hence, for the proposed sequence adaptation scheme, the required feedback bits per user is $QD + D \log_2(N)$. In the full-rank scheme, it is required to transmit QN bits per user. Hence, for the proposed scheme, the number of feedback bits can be decreased by a factor of $\frac{QD+D \log_2(N)}{QN}$. For $Q = 8$, $N = 16$ and $D = 5$ the reduction is around 50%, which is significant.

3. The proposed modification for an existing signature sequence optimization scheme

a. Transmitter and spreading sequence optimization scheme

In [10], Concha and Ulukus have considered a technique to optimize the transmitter powers as well as the signature sequences for users in a DS-CDMA system under multipath channel conditions. The optimality of the set of sequences is measured by the effective squared cross correlation among the sequences which is related to the achievable signal to interference plus noise ratio. The effective squared cross correlation TSC_{eff} is given by

$$TSC_{eff} = \sum_{i,j} |\tilde{\mathbf{s}}_i^H \tilde{\mathbf{s}}_j|^2, \quad 0 \leq i, j \leq K-1 \quad (3.16)$$

where $\tilde{\mathbf{s}}_i = \frac{\mathbf{H}_i \mathbf{s}_i}{\|\mathbf{H}_i \mathbf{s}_i\|}$. It is shown that, to achieve a common signal to interference ratio β such that $SINR_i > \beta$ for $0 \leq i \leq K-1$, β should satisfy the constraint $\beta \leq \frac{1}{\rho(\mathbf{A})}$, where $\rho(\mathbf{A})$ is the largest eigenvalue of \mathbf{A} and it is given by

$$(\mathbf{A})_{i,j} = \begin{cases} \left| \frac{\mathbf{s}_i^H \mathbf{H}_i^H \mathbf{H}_j \mathbf{s}_j}{\|\mathbf{H}_i \mathbf{s}_i\| \|\mathbf{H}_j \mathbf{s}_j\|} \right|^2, & \text{if } i \neq j \\ 0, & \text{otherwise.} \end{cases} \quad (3.17)$$

It can be easily derived that the quantity $\rho(\mathbf{A})$ is upper and lower bounded by, $\frac{1}{K}TSC_{eff} - 1 \leq \rho(\mathbf{A}) \leq \frac{1}{2}(TSC_{eff} - K)$. Hence, it can be assumed that it is reasonable to minimize TSC_{eff} to maximize $\frac{1}{\rho(\mathbf{A})}$ which allows β to have wider range of SINR.

It is also shown in [10] that, TSC_{eff} can be maximally decreased by updating each user's spreading sequence \mathbf{s}_k by

$$\mathbf{s}_k = \frac{1}{(\mathbf{v}^H \mathbf{D}^{-1} \mathbf{v})^{1/2}} \mathbf{U} \mathbf{D}^{-1/2} \mathbf{v}, \quad 0 \leq k \leq K-1 \quad (3.18)$$

where \mathbf{U} is the matrix with eigenvectors of $\mathbf{H}_k^H \mathbf{H}_k$ and \mathbf{D} is the corresponding diagonal matrix whose diagonal elements are the eigenvalues. Here, \mathbf{v} is the eigenvector of $\mathbf{D}^{-1/2} \mathbf{U}^H \mathbf{H}_k^H \mathbf{Z}_k \mathbf{H}_k \mathbf{U} \mathbf{D}^{-1/2}$ corresponding to the minimum eigenvalue, where

$$\mathbf{Z}_k = \sum_{j \neq k} \frac{\mathbf{H}_j \mathbf{s}_j \mathbf{s}_j^H \mathbf{H}_j^H}{\|\mathbf{H}_j \mathbf{s}_j\|^2}, \quad 0 \leq k \leq K-1. \quad (3.19)$$

TSC_{eff} can be reduced by evaluating the expression in (14) iteratively over all the users. Hence, by minimizing TSC_{eff} , $\frac{1}{\rho(\mathbf{A})}$ can be maximized such that $\beta < \frac{1}{\rho(\mathbf{A})}$. If the designed set of sequences can satisfy this condition, non-negative values for each user's transmitted power can be found by $\tilde{\mathbf{p}} = \beta \sigma^2 (\mathbf{I} - \beta \mathbf{A})^{-1} \mathbf{1}$, with $\tilde{\mathbf{p}} = [\tilde{p}_0, \tilde{p}_1, \dots, \tilde{p}_{K-1}]^T$ and $\tilde{p}_i = p_i \|\mathbf{H}_i \mathbf{s}_i\|^2$. The value p_i is the i th user's transmitted power.

However, it cannot be guaranteed that these p_i values are the optimum values

to achieve a given SINR. This is because, in the minimization of TSC_{eff} , only the normalized filtered spreading sequences are considered and the absolute power of the received filtered sequences has not been taken in to account. For example, for a given set of users' channels, one can design a set of spreading sequences which has the required TSC_{eff} . But, if the optimized set of spreading sequences does not exploit the channel gain properly, for some users, say \mathbf{s}_i , the energy of the received filtered sequence, $\mathbf{H}_i\mathbf{s}_i$, can be very low. Thus, to achieve a given SINR requirement, the required transmitted power $p_i = \tilde{p}_i/||\mathbf{H}_i\mathbf{s}_i||^2$ can be very high. Hence, we cannot guarantee that this optimization technique will give the set of spreading sequences that uses the optimum transmitter power to achieve a common SINR, β .

To overcome this, we propose to impose an additional constraint on the spreading sequences. This is done by representing each spreading sequence \mathbf{s}_k as $\mathbf{s}_k = \mathbf{F}_k\mathbf{a}_k$, where \mathbf{F}_k consist of D orthonormal basis vectors similar to that in the subsection A. That is, they are selected such that the basis vectors are the sinusoids which align with the strongest channel components of user k . With this constraint, we can guarantee that the received power of each user's spreading sequence will be considerably high.

With this constraint, the corresponding TSC_{eff} is given by

$$TSC_{eff} = \frac{\mathbf{s}_k^H \mathbf{H}_k^H \mathbf{Z}_k \mathbf{H}_k \mathbf{s}_k}{\mathbf{s}_k^H \mathbf{H}_k^H \mathbf{H}_k \mathbf{s}_k} + \kappa = \frac{\mathbf{a}_k^H \mathbf{G}_k^H \mathbf{Z}_k \mathbf{G}_k \mathbf{a}_k}{\mathbf{a}_k^H \mathbf{G}_k^H \mathbf{G}_k \mathbf{a}_k} + \kappa \quad (3.20)$$

where κ is independent of \mathbf{s}_k and $\mathbf{G}_k = \mathbf{H}_k \mathbf{F}_k$. After doing some matrix manipulation to (16), it can be shown that the optimum \mathbf{a}_k that reduces TSC_{eff} maximally is given by

$$\mathbf{a}_k = \frac{\mathbf{U}' \mathbf{D}'^{-1/2} \mathbf{v}'}{(\mathbf{v}'^H \mathbf{D}'^{-1} \mathbf{v}')^{1/2}}, \quad 0 \leq k \leq N-1 \quad (3.21)$$

where \mathbf{U}' and \mathbf{D}' are matrices with the same eigenvectors and the eigenvalues of $\mathbf{G}_k^H \mathbf{G}_k$. Here, \mathbf{v}' is the eigenvector of $\mathbf{D}'^{-1/2} \mathbf{U}'^H \mathbf{G}_k^H \mathbf{Z}_k \mathbf{G}_k \mathbf{U}' \mathbf{D}'^{-1/2}$ corresponding to

the minimum eigenvalue. It can be easily shown that

$$\mathbf{G}_k^H \mathbf{G}_k = \begin{bmatrix} \mathcal{H}_{k,1} & 0 & 0 & 0 & 0 & \dots \\ 0 & \mathcal{H}_{k,2} & 0 & 0 & 0 & \dots \\ 0 & 0 & \vdots & \vdots & \vdots & \dots \\ 0 & 0 & \vdots & \mathcal{H}_{k,r} & 0 & \dots \\ \vdots & \vdots & \vdots & \vdots & \vdots & \vdots \\ 0 & 0 & 0 & 0 & \dots & \mathcal{H}_{k,D} \end{bmatrix}.$$

where $\mathcal{H}_{k,r}$ is the r th strongest channel component of the k th user's channel.

Our proposed modification to the algorithm in [10] gives some additional advantages. As we have mentioned earlier, in the iterative algorithm in (3.18), \mathbf{D} is a diagonal matrix whose diagonal elements are the eigenvalues of $\mathbf{H}_k^H \mathbf{H}_k$. It is easy to show that, for a sufficiently large spreading sequence length N , the determinant of the matrix $\mathbf{H}_k^H \mathbf{H}_k$ is almost zero. In practice, \mathbf{H}_k is calculated by pilot symbols and the estimation of \mathbf{H}_k is imperfect due to the background noise. Hence, a small perturbation in the calculation of matrix $\mathbf{H}_k^H \mathbf{H}_k$ could make the matrix \mathbf{D} singular. But, in our proposed scheme, we always select the basis vectors according to the strongest channel components, and the resulting matrix $\mathbf{G}_k^H \mathbf{G}_k$ is always guaranteed to be non singular. Simulation results verify the convergence of our proposed algorithm.

b. Signature sequence optimization based on MMSE criteria

In the previous subsection, we have discussed the method of optimizing both transmitter power and the spreading sequence set. In [10], Concha and Uluks have also discussed a method of optimizing the spreading sequences for a fixed transmitted power. In this scheme, the optimized set of spreading sequences is obtained by updating the k th user's sequence in an iterative fashion according to

$$\mathbf{s}_k = \frac{1}{(\mathbf{z}_0^H \mathbf{D}^{-1} \mathbf{z}_0)} \mathbf{U} \mathbf{D}^{-1} \mathbf{z}_0, \quad 0 \leq k \leq K-1 \quad (3.22)$$

where \mathbf{U} and \mathbf{D} are the matrices with eigenvectors and eigenvalues of the matrix $\mathbf{I} + p_k \mathbf{H}_k^H (\mathbf{Z}_k + \sigma^2 \mathbf{I})^{-1} \mathbf{H}_k$ and \mathbf{z}_0 is the eigenvector of $\mathbf{D}^{-1/2} \mathbf{U}^H \mathbf{H}_k^H (\mathbf{Z}_k + \sigma^2 \mathbf{I})^{-2} \mathbf{H}_k \mathbf{U} \mathbf{D}^{-1/2}$ corresponding to the maximum eigenvalue. We can come up with a reduced-rank sequence updating algorithm by following the same line of arguments as in (3.18)-(3.19). The details of the approach will not be discussed here. Further, we can modify the transmitter and signature sequence optimization scheme discussed in the subsection 3.a to be used for signature sequence optimization under constrained transmitter powers, by fixing each user's transmitted power. Similar to the discussion in subsection 2.b, it can be easily shown that the proposed reduced-rank scheme requires fewer feedback overhead bits. To compare the performance of the transmitter and the signature sequence optimization scheme in [10] with the proposed subspace based optimization scheme (3.a), simulations were carried out with $\frac{1}{\sigma^2} = 5$ dB and $L = 2$. Here also we assume that each user's channel experiences frequency selective block fading and the performance is evaluated by averaging the users' performance in the given system over a large number of channel realizations. Dimensionality of the subspace is selected as $D = 3$. The number of users is 8 while the spreading length is 5. It can be seen from Fig. 11 that, at the low target SINR region, the proposed method requires less transmitter power than the scheme in [10] while it needs less transmitter power in the high SINR region. The reason for this behavior is that, with the additional power constraint on the proposed scheme, the achievable $\rho(\mathbf{A})$ value is higher than that of the scheme in [10]. Hence, according to 3.a, the corresponding target SINR region for which the system can perform well is much higher for the scheme in [10] than that of the proposed scheme. But, for a 12 user system with spreading sequence

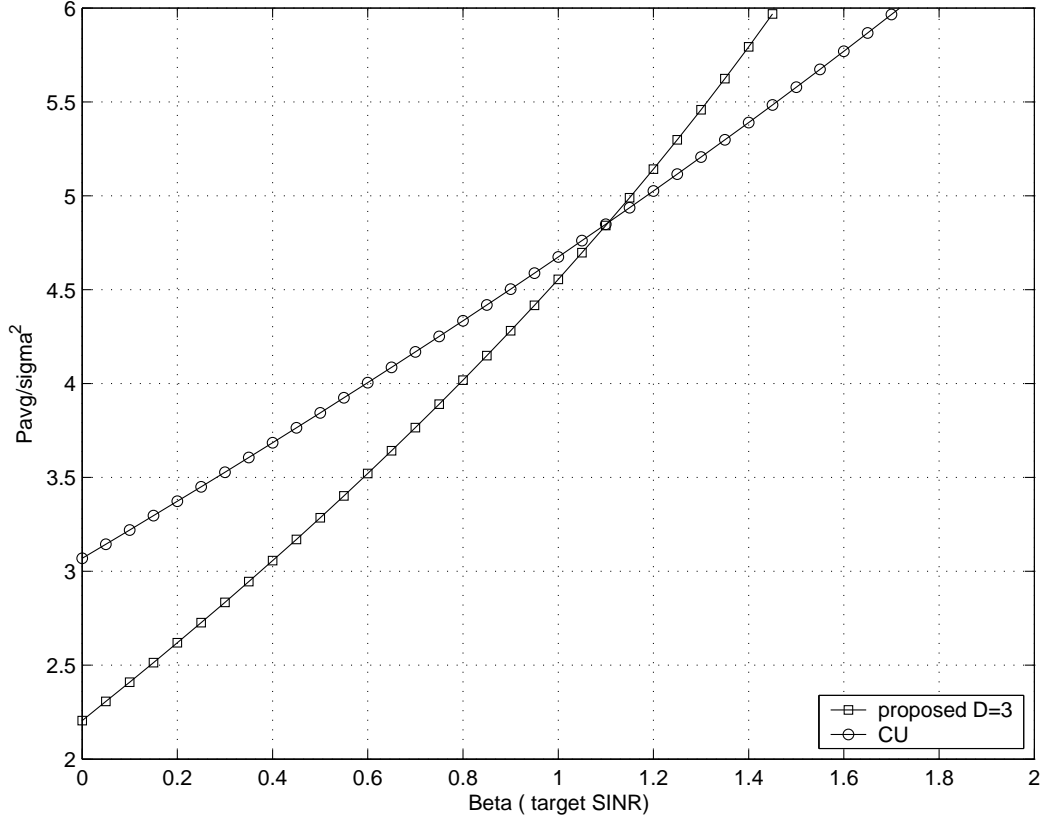


Fig. 11. Performance comparison of the transmitter power and spreading sequence optimization scheme [10] with the proposed reduced-rank version of it. CU=Concha and Ulukus [10]. $K=8$, $N=5$ and $L=2$. $\frac{1}{\sigma^2}=5$ dB.

length 16 and $D = 5$, which is a more practical situation, both the proposed and the system in [10] can achieve the lowest possible $\rho(\mathbf{A})$ value which is 0. The reason for the proposed system to achieve this minimum $\rho(\mathbf{A})$ value is, with $K \leq N$, there is much freedom to select a set of signature sequences that optimizes the cost function in (3.16). Thus, the SINR region that both systems successfully operate in is $[0, \infty)$. Hence, with the additional power optimization strategy, the proposed system outperforms the one in [10]. The simulation results in Fig. 12 verify this by illustrating that, the required average transmitter power for the proposed scheme is always 5 dB

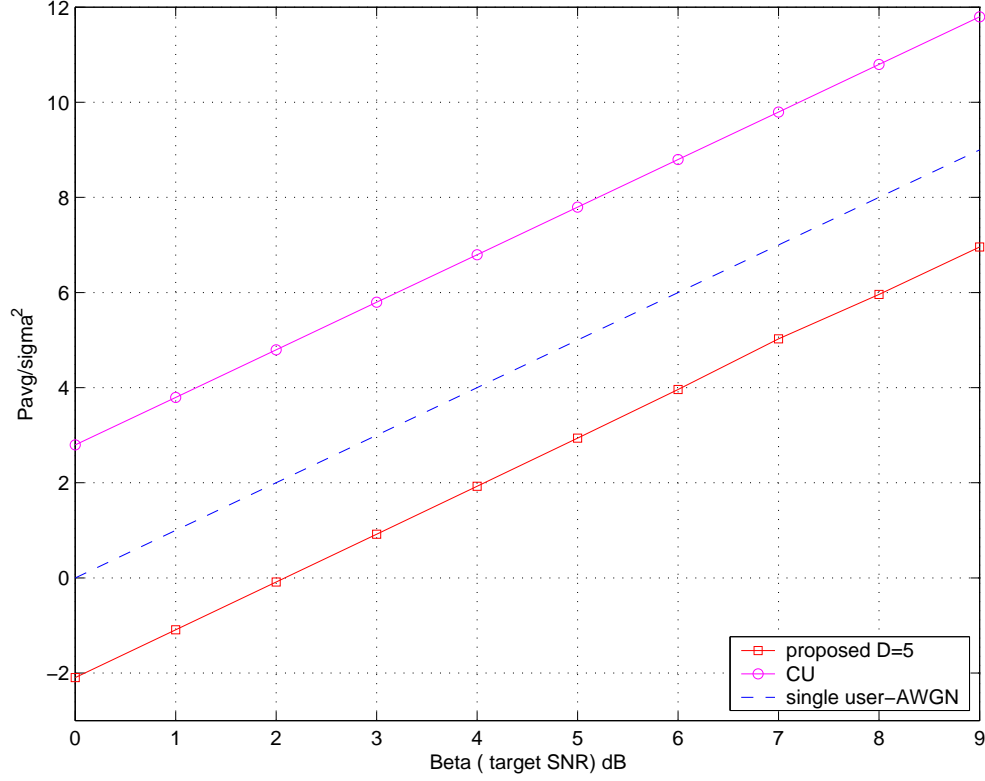


Fig. 12. Performance comparison of the transmitter power and spreading sequence optimization scheme [10] with the proposed reduced-rank version of it. CU=Concha and Ulukus [10]. $K=12$, $N=16$ and $L=2$. $\frac{1}{\sigma^2}=5$ dB.

less than that of the transmitter and signature sequence optimization scheme in [10]. Fig. 13 and Fig. 14 compare the performance of MMSE based sequence optimization scheme in [10] with the proposed reduced-rank MMSE sequence optimization scheme. It can be seen that both schemes perform equally well; note however, that the proposed schemes uses only the 5 strongest frequency components. The figures further show that, when we fix the transmitter power and use the proposed reduced-rank transmitter and receiver optimization scheme (3.a), the performance of the system is almost the same as that of the MMSE based sequence optimization scheme (refer to

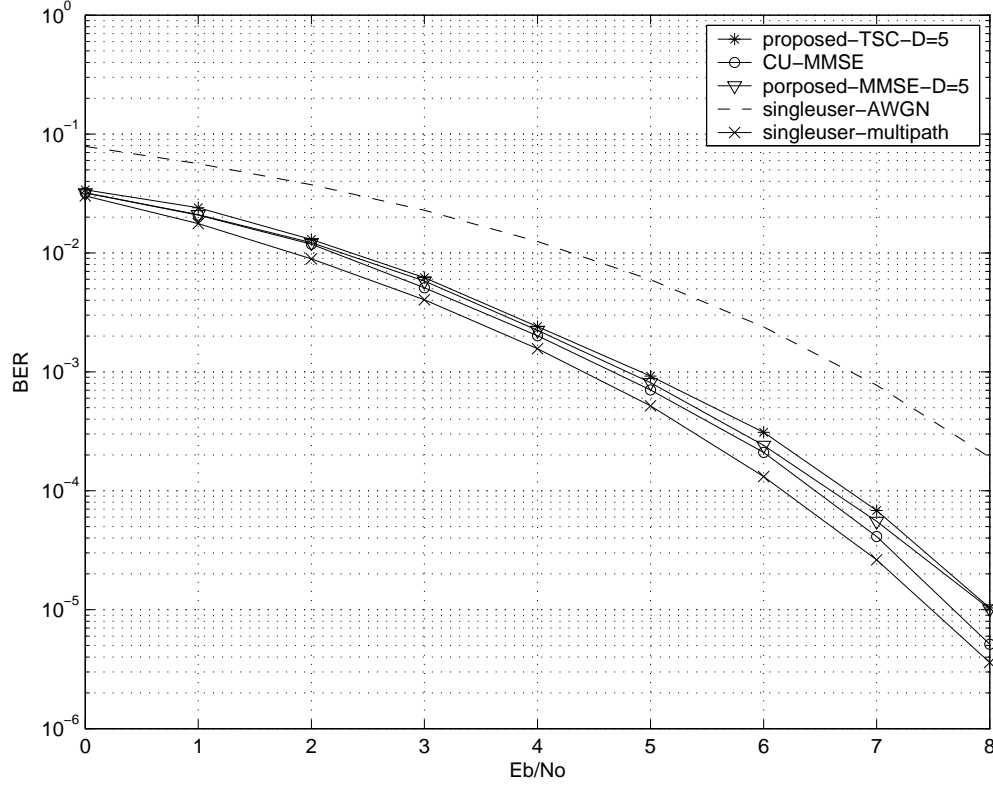


Fig. 13. Performance comparison of MMSE sequence optimization scheme [10] with the proposed reduced-rank version of it. CU=Concha and Ulukus [10]. Uplink is considered. $K=12$, $N=16$ and $L=2$.

3.b). It can be further seen (compare with Fig. 9 and Fig. 10) that, the performance of the reduced-rank MMSE sequence optimization scheme is very close to that of the transmitter adaptation scheme (Rajappan and Honig).

In this chapter, we have proposed a frequency domain approach to design a set of spreading sequences for a DS-CDMA system in the presence of frequency selective fading. We showed that the number of parameters involved in the design of optimal spreading sequences can be made smaller when they are analyzed in the frequency domain, than when they are analyzed in the time domain. Further, it was shown that

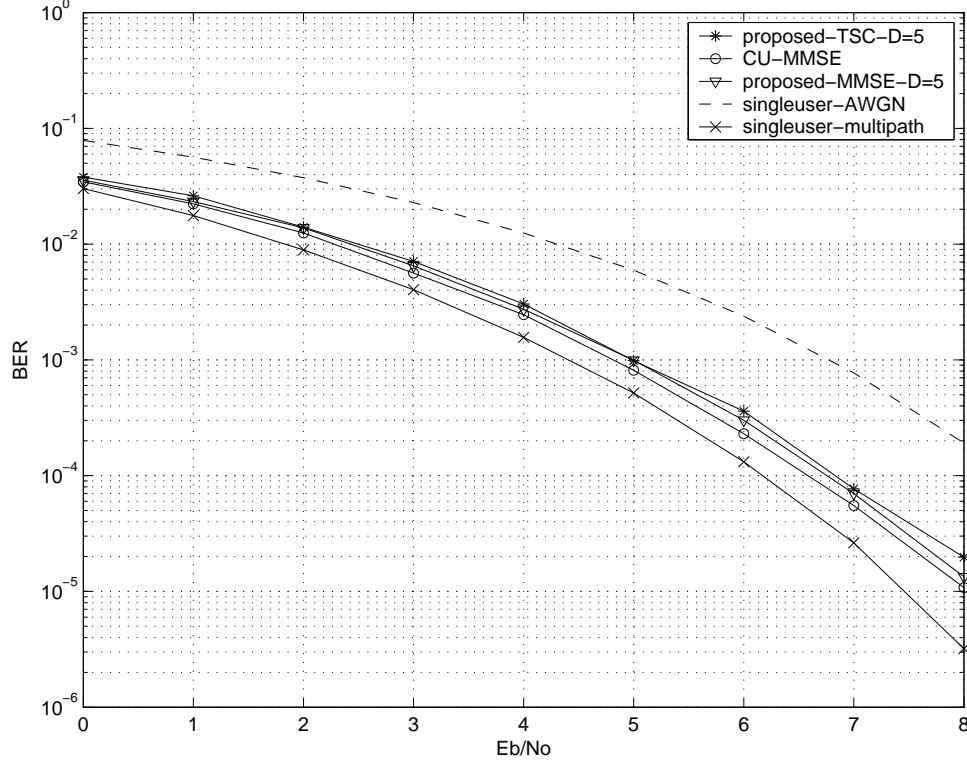


Fig. 14. Performance comparison of MMSE sequence optimization scheme [10] with the proposed reduced-rank version of it. CU=Concha and Ulukus [10]. Downlink is considered. $K=12$, $N=16$ and $L=2$.

for multipath channels, designing a set of spreading sequences in the frequency domain reduces to assigning a spreading sequence for each user with a spectrum whose spectral lines are located at the strongest spectral components of the users channels spectrum while keeping the cross correlation at a very low value for spreading sequences with overlapping spectra. We have also showed that by designing spreading sequences in the frequency domain, the performance of some existing algorithms for the design of spreading sequences can be improved and/or the computational complexities can be reduced.

CHAPTER IV

THE DESIGN OF CONSTRAINED AMPLITUDE SPREADING SEQUENCES
USING SPECTRAL DOMAIN PROPERTIES

In the previous chapter, we have discussed the design of spreading sequences for frequency selective channels by exploiting the users' channel state information. There, the designed sequences have shown superior performance over that of the conventional sequence design schemes and also have outperformed the single user AWGN channel performance.

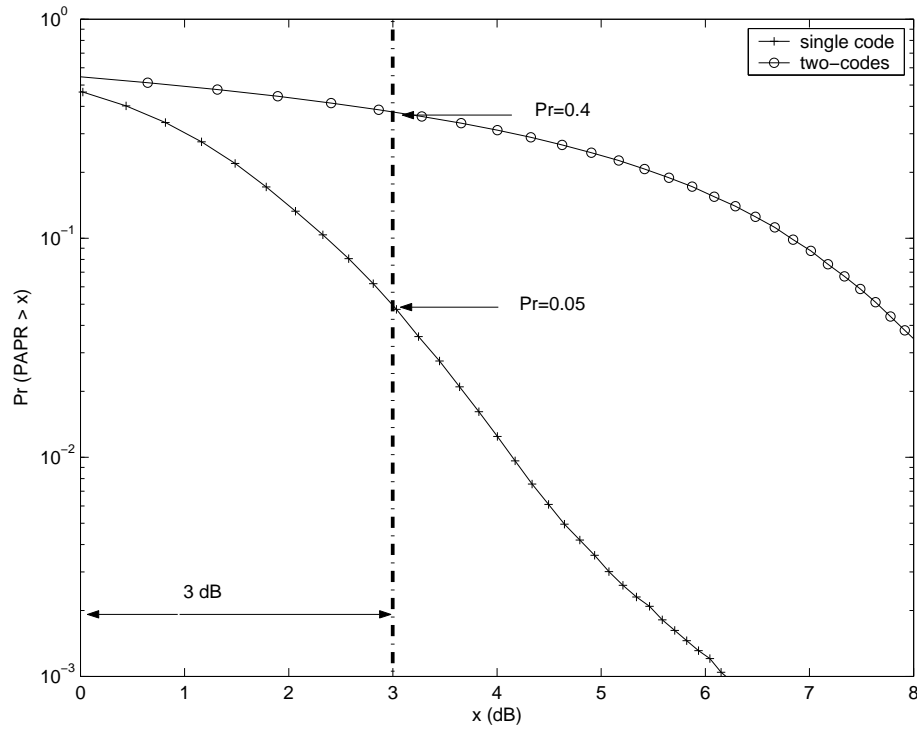


Fig. 15. PAPR distributions of single code and multi-code DS-CDMA signals.

Unfortunately in almost all the proposed algorithms, the designing has been done with the assumption that the chips of the sequences have unconstrained ampli-

tudes and phases. There are many disadvantages of using unconstrained sequences in a DS-CDMA system. First, once the sequences are designed at the designed end (transmitter/receiver), the sequences have to be transmitted to the other end (receiver/transmitter) of the communication channel. This demands a considerable feedback bandwidth. Secondly, unconstrained sequences have high peak to average power ratio (PAPR) at the transmitter output. For example, in Fig. 15 we have plotted the PAPR distributions of single code and multi-code systems, where the spreading sequences are optimized according to the scheme proposed in [9]. It can be seen that, when each user is allowed to use a single spreading sequence, 5% of the time, the PAPR is greater than 3 dB at the user's transmitter output. If the system supports users to use multiple spreading sequences, the PAPR could be much higher. For example, when users are allowed to use two spreading sequences, more than 40% of the time, the PAPR is greater than 3 dB. This high PAPR demands a wider dynamic range of the transmitter amplifier increasing the cost of the amplifier. Hence, we can see that there is a considerable demand for the design of constrained amplitude sequences for CDMA systems.

In this chapter, we capitalize the observation in Chapter III that the spectra of the spreading sequences designed according to existing algorithms are narrowband and are located at the strongest spectral components of the users' channels to design constrained amplitude sequences for frequency selective channels.

A. Constrained amplitude sequence design

1. Constrained amplitude sequence design by mapping unconstrained sequences onto a unit circle

If we restrict the chips of the spreading sequences to have a unit amplitude, the optimization problem is a solution to

$$\max \gamma_k \text{ s.t. } |\mathbf{s}_{k,q}| = \sqrt{(p/N)}, \quad 0 \leq q \leq N-1 \quad (4.1)$$

where γ_k is the received SINR of the k th user and $\mathbf{s}_{k,q}$ is the q th chip of the spreading sequence \mathbf{s}_k . The optimization problem in (4.1) is equivalent to the optimization problem in (3.5) except the constraint imposed on each chip of the spreading sequence \mathbf{s}_k .

This kind of an optimization is intractable in general [35]. To circumvent this problem, we first relax the constraint imposed on the chips of the spreading sequences and perform the unconstrained optimization proposed in [9]. Then, at each iteration, we simply project the chips of the optimized unconstrained spreading sequences onto a unit circle. That is, in each user iteration, the k th user's optimized sequence \mathbf{s}_k is replaced by a unit circle sequence where the q th chip of the spreading sequence \mathbf{s}_{UNITk} which is $\mathbf{s}_{UNITk,q}$ is given by

$$\mathbf{s}_{UNITk,q} = \exp(j \arg[\mathbf{s}_{k,q}]), \quad 0 \leq q \leq N-1. \quad (4.2)$$

The unit circle mapping allows to reduce the PAPR. But, since the phases of the chips of a unit circle sequences can take any value between 0 and 2π , to transmit the phase information it requires a considerable amount of feedback bits. For example, if we quantize each chip's phase with A bits, the required number of feedback bits is $A \times N$. Instead of directly quantizing phases of the chips, we propose the following algorithm.

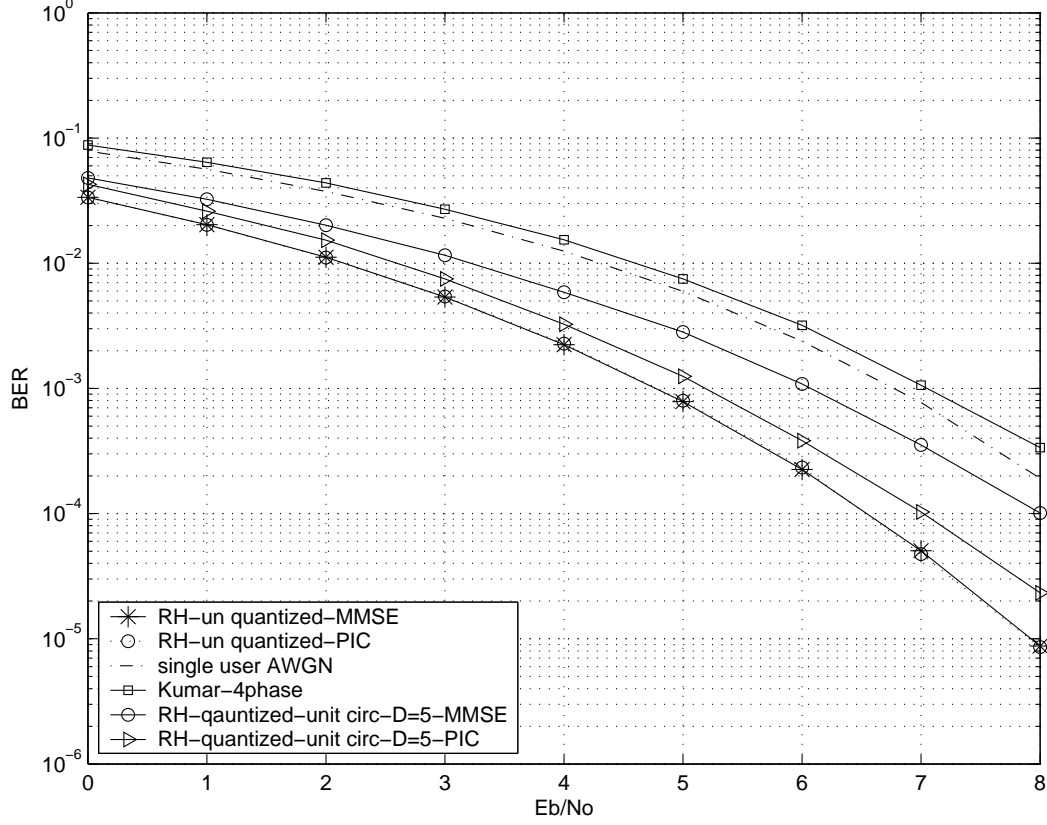


Fig. 16. The performance of the unit circle sequences with frequency domain quantized coefficients. $K=12$, $N=16$. RH-quantized = Sequences designed according to (3.13) with quantized $\alpha_{k,r}$. RH-unquantized = Sequences designed according to (3.13) with unquantized $\alpha_{k,r}$ and $D = N$.

First, we observe the narrowbandness of each spreading sequence \mathbf{s}_k and represent \mathbf{s}_k with a reduced number of basis vectors (say D) according to (3.11) and (3.13). Then we do the optimization to find the optimum basis vector coefficients $\alpha_{k,r}$ s for each user. Secondly, we quantize the coefficients $\alpha_{k,r}$ s of the basis vectors with Q bits before mapping the reconstructed \mathbf{s}_k onto a unit circle sequence. That is, if the quantized coefficients of the basis vectors for the k th user's spreading sequence are $\hat{\alpha}_{k,r}$ s, then the corresponding unit circle sequence is given by $\hat{\mathbf{s}}_{UNITk} = \exp(j \arg(\sum_{r \in I} \hat{\alpha}_{k,r} \mathbf{f}_r))$. Note that D and Q are selected such that the required number of overhead bits $Q \times D$

is as small as possible while the performance of the reduced-rank quantized sequences is very close to that of full rank unquantized sequences.

It should be noted that to reconstruct the unit circle sequences both at the receiver and the transmitter, it needs only the information of the quantized coefficients $\hat{\alpha}_{k,r}$ s of the basis vectors. Hence, it is sufficient to transmit only $\hat{\alpha}_{k,r}$ s from the designed end to the other end of the communication channel (transmitter/receiver) and no additional information has to be transmitted regarding the phases of the chips.

To verify the performance of the proposed unit circle sequences, simulations were carried out for a DS-CDMA system. Each user's channel is assumed to be a 2-tap frequency selective channel where taps are drawn from a Gaussian distribution and the power is normalized to one. Very slow fading similar to that of in [9], [32] is assumed and therefore, in the simulations the channels do not change over the time duration required to design the spreading sequence and feed it back. Spreading sequence length is 16 and the number of users is 12 corresponding to a 75% loading.

Fig. 16 shows the performance of an uplink DS-CDMA system with chips of the spreading sequences mapped onto a unit circle according to the subsection 1 in section A. For comparison, we have also included the single user performance in an AWGN channel, performance of the un-quantized sequences ([9], $D = N$) and the performance of the complex sequences proposed in [36]. Since it requires at least $2N$ bits to represent any complex spreading sequences (e.g. QPSK), to make a fair comparison between the unit circle sequences and any other type of complex sequences, we have selected D and Q such that $D = 5$ and $\alpha_{k,r}$ is uniformly quantized with 3 bits per dimension. Hence, the required number of feedback bits is almost $2N$. It can be seen that with the use of a parallel interference canceller and an MMSE detector, the performance of the unit circle sequences is 0.5 dB and 1.4 dB away from that of the un-quantized sequences. It also shows that, even with the MMSE

receiver, unit circle sequences outperform single user AWGN performance. This is because, each user's unit circle sequence is designed to exploit that user's channel gain. Performance of the complex sequences proposed in [36] is 0.8 dB away from that of the proposed unit circle sequences.

2. The design of constrained amplitude sequences using already existing family of sequences

As discussed in Chapter III, it is possible to design nearly optimum spreading sequences for multipath channels by assigning spreading sequences with narrowband spectra centered around the strongest channel frequencies, while maintaining a low cross correlation among the sequences that have overlapping frequency spectra. If it is possible to design a set of spreading sequences with fixed amplitude chips with the above given characteristics then, that set will provide good performance while maintaining a reduced feedback bandwidth and a low PAPR at the transmitter output.

To tackle this problem we first select a subset of spreading sequences from the set of Oppermann sequences. An Oppermann sequence [37] is a unit amplitude sequence where the members of the spreading sequence set are given by

$$\mathbf{o}_i^M = (-1)^{iM} \exp \left[\frac{j\pi(M^m i^p + i^n)}{N} \right], \quad 0 \leq M, i \leq N - 1, \quad (4.3)$$

where m, p, n are any real numbers. The triple $\{m, p, n\}$ specifies the sequence set and the M refers to the M th sequence in the family. It is shown in [37] that, if p is set to 1, all the sequences will have the same autocorrelation magnitude. Hence, the corresponding spectra will have the same shape while localized at different frequencies. Further, it is shown that if N is prime, correlation between any two sequences in the same family is zero. We select the Oppermann sequences with $p = 1$ and $m = 1$ and vary n until we get a set of spreading sequences whose spectra are narrow band and

centered around N different discrete frequency points. If we assign these spreading sequences for users such that each user's strongest channel frequency matches with the center frequency of the spreading sequence, we can guarantee that the received filtered sequences will also have low cross correlation properties. The reason for this is that, since the spreading sequences are narrow band sequences, after filtering through the corresponding channels, the received filtered sequences will also have spectra close to those of the transmitted sequences. But this assignment of spreading sequences is not always possible since there is a possibility that two or more users may have the same strongest channel frequency. We have developed the following strategy for assigning sequences for such users. (For this technique, we select two sets of Oppermann sequences with narrow band spectra given by $\{\mathbf{o}_i^1\}$ and $\{\mathbf{o}_i^2\}$, $0 \leq i \leq N - 1$).

Let the k th user's channel be \mathbf{h}_k and the corresponding frequency indices of the user's r strongest channel components be $[l_{k1}, l_{k2}, \dots, l_{kr}]$.

1. For the k th user's channel \mathbf{h}_k , select the corresponding Oppermann sequence \mathbf{o}_j^1 , such that $\mathcal{F}(\mathbf{o}_j^1) = l_{k1}$ (we define \mathcal{F} as the operator that gives frequency index of the strongest frequency of a sequence). If the selected sequence \mathbf{o}_j^1 has not been assigned for the users $1, \dots, k - 1$, assign that sequence for the k th user.
2. If the selected sequence \mathbf{o}_j^1 has previously been assigned to a user u with channel \mathbf{h}_u then, we search the second set of Oppermann sequences \mathbf{o}^2 and select the Oppermann sequence \mathbf{o}_m^2 such that $\mathcal{F}(\mathbf{o}_m^2) = \mathcal{F}(\mathbf{o}_j^1) = l_{k1}$. This guarantees that the received power at the k th user's receiver is high. But, since the sequences of the users k and u are not from the same Oppermann sequence set, the cross correlation between the two users is not necessarily small. To reduce the cross

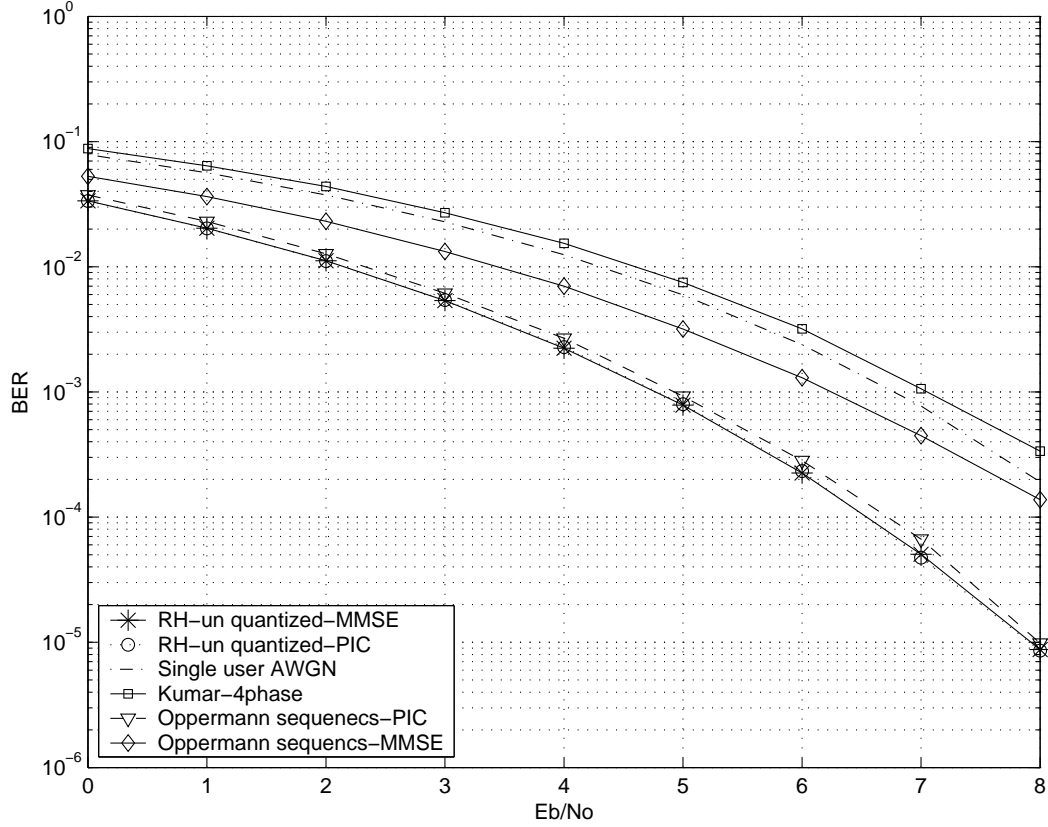


Fig. 17. Performance of the Oppermann sequences. $K=12$, $N=15$. Uplink is considered.

correlation, we multiply the k th user's Oppermann sequence by $e^{j\theta}$ so that the spreading sequence for user k is given by $\mathbf{o}_m^2 e^{j\theta}$. The angle θ is selected such that the real part of the cross correlation between the filtered sequences of the users k and p is zero. That is $\Re[\tilde{\mathbf{o}}_j^H \tilde{\mathbf{o}}_m^2 \exp(j\theta)] = 0$. Where $\tilde{\mathbf{o}}_j^1 = \mathbf{h}_p \odot \mathbf{o}_j^1$ and $\tilde{\mathbf{o}}_m^2 = \mathbf{h}_k \odot \mathbf{o}_m^2$. \odot is the convolution operation. The value of θ is given by, $\theta = \tan^{-1}[\Re(\tilde{\mathbf{o}}_j^H \tilde{\mathbf{o}}_m^2) / \Im(\tilde{\mathbf{o}}_j^H \tilde{\mathbf{o}}_m^2)]$. Note that this is possible only if \mathbf{o}_m^2 has not been assigned previously. The algorithm does not optimize more than two users at a time since optimization with more users leads to an increase in the complexity of the algorithm.

3. If both \mathbf{o}_j^1 and \mathbf{o}_m^2 have been assigned previously, then select an unassigned Oppermann sequence \mathbf{o}_q^1 from the set \mathbf{o}^1 such that $\mathcal{F}(\mathbf{o}_q^1) = l_{ki}$ for $2 \leq i \leq N - 1$. The selection should be done such that the algorithm searches for the next strongest channel frequency l_{kr} in the descending order.
4. Carry out this for all the users in the system.

From the above given algorithm, it is possible to obtain a set of spreading sequences whose filtered outputs have smaller cross correlation while producing sufficiently high SNR output at the receiver. Further, the optimization here reduces to optimizing the performances of two users (k and u) at a time rather than optimizing all N users jointly. The latter is prohibitively complex for a set of spreading sequences with fixed amplitude chips. Another advantage of using Oppermann sequences is that only $\{M, m, n, \theta\}$ need to be sent from the transmitter to the receiver if the optimization is centralized.

Fig. 17 shows the performance of the system when the chips of the spreading sequences are derived from a subset of Oppermann sequences. These spreading sequences are from the selected subset of Oppermann sequences with $N=15$. Here, n has been varied to obtain two families of orthogonal narrow band sets of sequences as discussed in this subsection. Simulation conditions are the same as that of in subsection 1, section A. It can be seen from Fig. 17, the proposed scheme to design spreading sequences with a fixed amplitude alphabet provides a 1.6 dB gain over the single user AWGN performance with the use of a PIC. The proposed scheme also provides 2 dB gain over complex sequences proposed in [36]. Further, the performance of the system with Oppermann sequences is only a few tenths of a dB away from that of the unconstrained sequences. Even with the use of an MMSE receiver, the unit circle sequence outperforms AWGN performance and the complex sequences proposed in

[36] by about 0.4 dB and 0.7 dB respectively.

CHAPTER V

THE DESIGN OF FINITE ALPHABET SPREADING SEQUENCES BASED ON THE WATERFILLING CONCEPT

In the previous chapter, we mainly discussed the design of spreading sequences with constrained amplitude chips which was helpful to reduce the PAPR at the transmitter output over that of the unconstrained spreading sequences.

In this chapter, we focus on the design the spreading sequences not only with constrained amplitude chips but also with chips derived from a finite alphabet. Here, we restrict the alphabet of the chip sequences to be from a QPSK constellation. In this design, we consider two cases - (i) knowledge of the channel state information (CSI) of all the users is available centrally during the design process such as at the base station (ii) the design is at the mobile unit when each user knows only the CSI of his/her frequency selective channel. In both cases, we propose novel techniques to design spreading sequences whose spectra are well matched to the waterfilling spectrum of the frequency selective channel. In the former case, a set of short spreading sequences is designed that is both well matched to the frequency selective channels and possesses a low cross correlation. In the latter case, the use of long spreading sequences and error control coding is proposed. The sequences that follow the waterfilling spectra are obtained by considering that the sequences are to be from the outputs of appropriately designed Markov sources.

A. Design of spreading sequences

For our analysis, we consider the system model in (2.2) which is given by

$$r_{q,m} = \sum_{k=0}^{K-1} \sum_{j=0}^{L-1} x_{k,m} s_{k,q-j} h_{k,j} + n_q, \quad 0 \leq q \leq N-1. \quad (5.1)$$

If we represent (5.1) in terms of filtered chip sequences $\mathbf{f}_k = \mathbf{s}_k \odot \mathbf{h}_k$, where \odot denotes the convolution, it becomes

$$r_{q,m} = \sum_k x_{k,m} f_{k,q} + n_q \quad (5.2)$$

where $f_{k,q}$ is the q th element of \mathbf{f}_k . The SINR at the front end of the k th user's matched filter receiver is given by

$$\begin{aligned} \text{SINR}_k &= \frac{||\mathbf{s}_k \odot \mathbf{h}_k||^2}{\sum_{j \neq k} ||\mathbf{s}_j \odot \mathbf{h}_j||^2 + \sigma^2} \\ &= \frac{||\mathbf{f}_k||^2}{\sum_{j \neq k} ||\mathbf{f}_j||^2 + \sigma^2}. \end{aligned} \quad (5.3)$$

1. Basic idea

In Chapter III, we have shown that the power spectrum of a user's spreading sequence that tries to maximize the user's SNR should be narrowband and lies very close to the strongest spectral components of the channel. But, in a multiuser environment an additional care has to be taken to design the users' sequences to reduce the cross correlation effect. the best way to do this is to jointly optimize the sequences that minimize a global cost function. For an uncoded system, the cost function is the sum of mean squared error of all the user's information bits. This optimization is handled in an iterative fashion in [9] where each user tries to maximize that user's SNR while avoiding interference from other users.

But, for a coded system, it is shown in information theory that the sum capacity of a multiuser system is achieved by way of multiuser waterfilling [38]. In terms of design of spreading sequences, optimal long spreading sequences are those whose spectra are obtained according to the multiuser waterfilling. Although waterfilling across the users is the optimal technique to achieve the sum capacity, practically this is very complex and an iterative technique is required [39]. Further, since the multiuser

waterfilling is optimal only asymptotically in the length of spreading sequences, it is not straightforward to design good short spreading codes based on the multiuser water filling. As an alternative but sub optimal approach, we design the users' spreading sequences such that each user's spreading sequence is well matched to the single user waterfilling spectrum. Here, each user's spreading sequence is obtained at the output of a Markov source with an appropriately chosen probability transition matrix. Once a set of single user spreading sequences are designed for each user's channel we select the optimum set, one code from each user, such that the cross correlation among the users' spreading sequences are minimized. It should be noted that, this proposed technique is not restricted only to the sequences that follows the waterfilling spectrum. Generally, we can design a set of spreading sequences that require given spectral characteristics with very low cross correlation properties. For example, for an uncoded system, the sequences should be designed such that spectrum of each user's spreading sequence is a narrowband one centered at the strongest spectral components of the channel.

2. Single user design

In the absence of the other users, the received signal at the k th user's matched filter is given by

$$y_{k,q} = \sum_{j=0}^{L-1} h_{k,j} s_{k,q-j} + n_q, \quad 0 \leq q \leq N-1. \quad (5.4)$$

It is shown in [40] that, for a discrete-time Gaussian channel, the spectrum $\epsilon_k = (\epsilon_{k,0}, \epsilon_{k,1}, \dots, \epsilon_{k,N-1})$ of the capacity achieving sequence \mathbf{s}_k should satisfy

$$\epsilon_{k,q} = \begin{cases} \frac{N_0}{2}(\theta - |H_{k,q}|^{-2}), & \text{if } \theta |H_{k,q}|^2 > 1 \\ 0, & \text{otherwise} \end{cases} \quad (5.5)$$

where $(H_{k,0}, H_{k,1}, \dots, H_{k,N-1})$ is the discrete-time channel frequency spectrum given

by

$$H_{k,q} = \sum_{p=0}^{N-1} h_{k,p} e^{-j2\pi pq/N}, \quad 0 \leq q \leq N-1. \quad (5.6)$$

Here, θ is a parameter given by

$$\sum_{q=0, H_{k,q} \neq 0}^{N-1} \max(\theta - |H_{k,q}|^2, 0) = 2NE_s/N_0 \quad (5.7)$$

where E_s is the chip energy. From (5.5)-(5.7) the required waterfilling spectrum of the particular channel can easily be found. It should be noted that the channel coefficients of the low pass equivalent model of a practical multipath channel are complex. Hence, the desired waterfilling spectrum is not necessarily symmetric about zero frequency. It is impossible to match this asymmetric waterfilling spectrum with a real valued spreading sequence which can only provide a symmetric power spectrum. To achieve this spectrum, it is necessary to use a complex valued spreading sequence having a certain degree of correlation between real and imaginary parts of the sequence.

In our approach, for user k , we first generate a long complex valued sequence (much longer than the spreading length) $\mathbf{S}_k = \{s_{k,j}\}_{j=1}^t$ of length t that possesses the desired spectrum. As a computationally efficient method, we consider \mathbf{S}_k to be an output of a Markov chain with a given probability transition matrix (PTM). In our simulation we generate \mathbf{S}_k with QPSK signals derived from the constellation $\mathbf{c} = [c_0, c_1, c_2, c_3]^T$ with $c_m = e^{j(2m+1)\pi/4}$ for $0 \leq m \leq 3$, according to the probability transition matrix given below

$$\mathbf{P} = \begin{pmatrix} p_{11} & p_{12} & p_{13} & p_{14} \\ p_{21} & p_{22} & p_{23} & p_{24} \\ p_{31} & p_{32} & p_{33} & p_{34} \\ p_{41} & p_{42} & p_{43} & p_{44} \end{pmatrix}.$$

Here, p_{ml} for $0 \leq m \leq 3$ and $0 \leq l \leq 3$ denotes the probability that the symbol c_l is

selected as the output in a given interval, given that the symbol c_m is selected in the previous interval. If the autocorrelation function of the generated Markov sequence is given by $\hat{R}(q)$, where q is the time index, then it can be shown that

$$\begin{aligned}\hat{R}(q) &= E[s_{k,n} s_{k,n+q}^*] \\ &= \sum_{m,l} c_m c_l^* \Pr(s_{k,n} = c_m, s_{k,n+q} = c_l)\end{aligned}\quad (5.8)$$

where $s_{k,n}$ is the n th chip of the k th user's Markov sequence and $*$ denotes complex conjugate. We can rearrange (5.8) as

$$\begin{aligned}\hat{R}(q) &= \sum_{m,l} c_m c_l^* \Pr(s_{k,n} = c_m) \Pr(s_{k,n+q} = c_l | s_{k,n} = c_m) \\ &= \frac{1}{4} \sum_{m,l} c_m c_l^* \mathbf{P}_{m,l}^q\end{aligned}\quad (5.9)$$

where $\mathbf{P}_{m,l}^q$ is the m th row l th column element of \mathbf{P}^q (\mathbf{P} is the PTM). Here, we have assumed that each symbol in the constellation is equiprobable. After rearranging the terms inside the summation, it can be easily shown that the autocorrelation $\hat{R}(q)$ of the complex valued Markov sequence with a given PTM is given by

$$\hat{R}(q) = \frac{1}{4} \mathbf{c}^H \mathbf{P}^q \mathbf{c}. \quad (5.10)$$

If the autocorrelation function of the desired spectrum (waterfilling spectrum) is $R(q)$, we can find a suitable PTM that generates the longer complex sequences \mathbf{S}_k , which approximately matches the desired waterfilling spectrum in the mean squared sense by

$$\hat{\mathbf{P}} = \arg \min_{\mathbf{P}} \sum_q |\hat{R}(q) - R(q)|^2. \quad (5.11)$$

Fig. 18 illustrates an example of this method for a channel with channel coefficients given by $\mathbf{h}_k = [0.6381 - 0.5252j, -0.5323 + 0.1834j]$. It can be seen from the figure that, the power spectrum of a sequence that is generated as an output of an

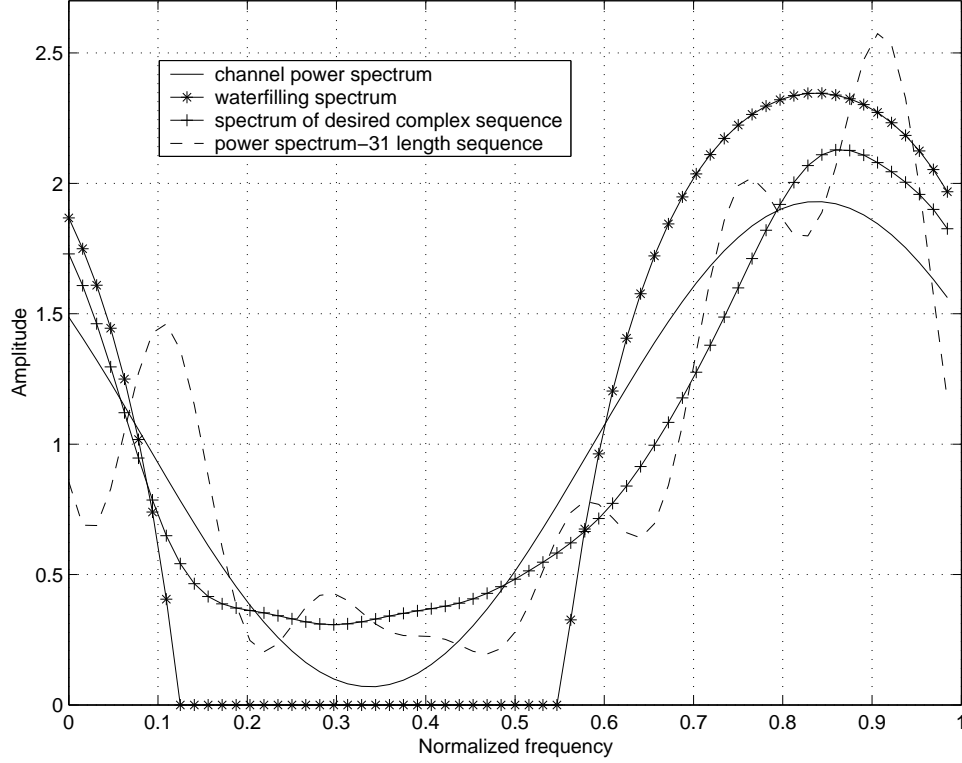


Fig. 18. Comparison of the waterfilling spectrum with the spectrum of the complex sequence generated by an appropriate first order Markov chain.

appropriate Markov chain and the power spectrum of a 31 length sequence derived from that Markov sequence closely follows the waterfilling spectrum of the channel.

3. Selection of the optimal short spreading sequences

In designing of short spreading sequences, we assume that the knowledge of each user's CSI is available centrally. Fig. 19 illustrates the selection procedure of short spreading sequences from the long Markov sequence. Here, for user k , a set of spreading sequences of length N is obtained from \mathbf{S}_k according to $\mathbf{s}_k^n = [s_{k,n}, s_{k,n+1}, \dots, s_{k,n+N-1}]^T$. The selected \mathbf{s}_k^n sequences are the best ones in the sense that, the MSE between the desired waterfilling spectrum of the k th user's channel and the spectrum of \mathbf{s}_k^n is

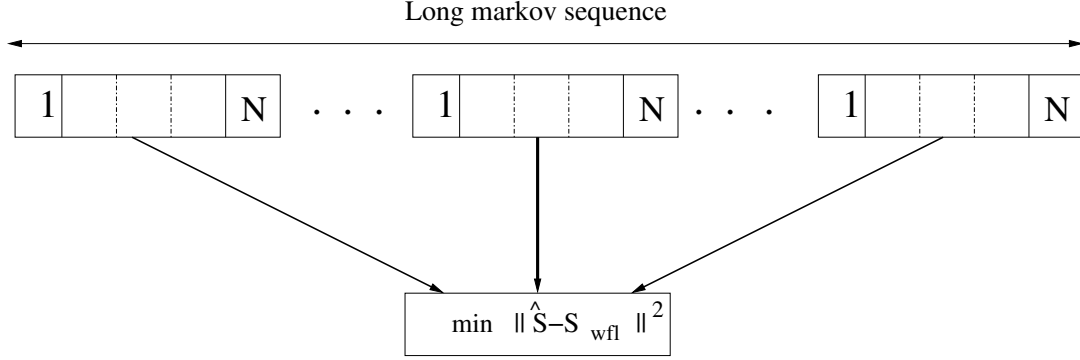


Fig. 19. Figure that illustrates the selection procedure of short spreading sequences from the long Markov sequence.

higher than that of the rest of the sequences in \mathbf{S}_k . In simulations, we have selected the best 5% sequences in \mathbf{S}_k . Once the set of good sequences for each user is found we have to select a set of K sequences which includes one spreading code from each single user's spreading code set that minimizes the overall BER of the system with the use of a suitable multiuser detector. This is similar to the selection of spreading sequences such that each user experiences a minimum interference from other users.

Here, we explain a procedure to perform this minimization. Let the k th user's filtered spreading sequence \mathbf{f}_k be given by, $\mathbf{f}_k = [f_{k,0}, f_{k,1}, \dots, f_{k,N-1}]^T$. We define the matrix \mathbf{F} of filtered spreading sequences as $\mathbf{F} = [\mathbf{f}_1 \mathbf{f}_2 \dots \mathbf{f}_K]^T$. Then, the corresponding correlation matrix among the filtered sequences is given by $\mathbf{R} = \mathbf{F}^H \mathbf{F}$. It can be shown that R_{kk} and $\sum_{p=0, p \neq k}^{K-1} R_{kp}$ gives the signal and interference components of the k th user at the receiver after despreading the received signal using the k th user's filtered spreading sequence \mathbf{f}_k . Here, R_{ij} is the i th row j th column element of the matrix \mathbf{R} . To select a set of spreading codes that have minimum interference among the users, the following steps are followed (see Fig. 20).

1. Randomly select a sequence \mathbf{s}_k from each user k to form a set of sequences

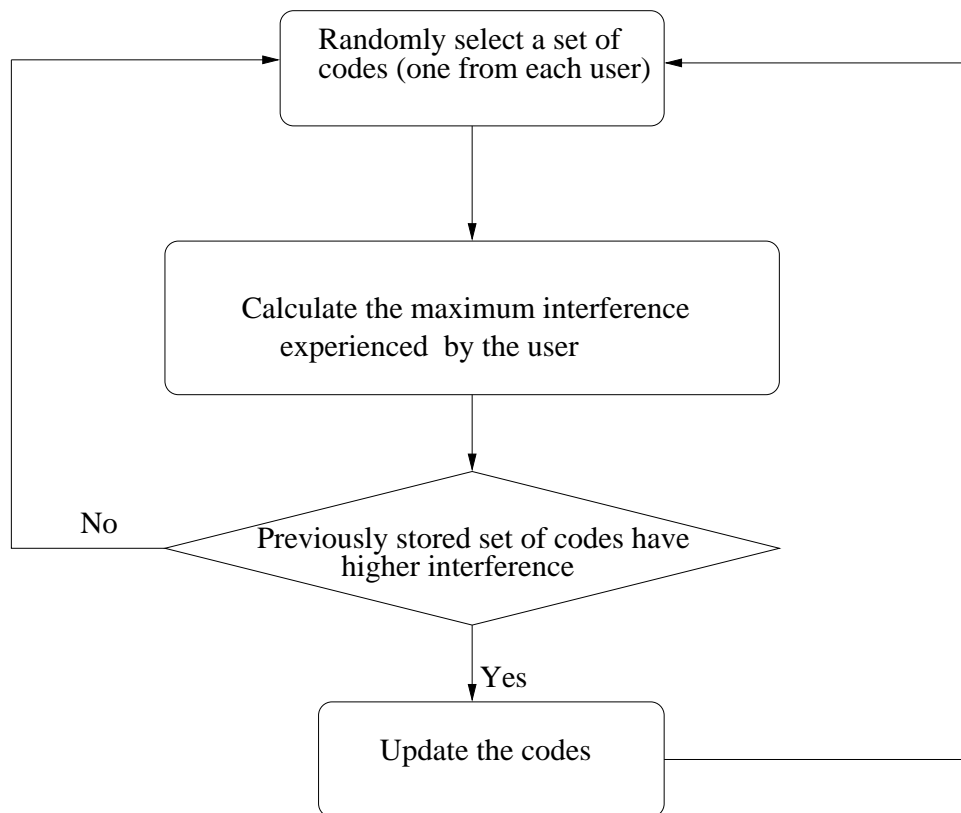


Fig. 20. Flow chart to find a set of spreading sequences with low cross correlation properties.

- $\mathbf{S} = [\mathbf{s}_0, \mathbf{s}_1, \dots, \mathbf{s}_{K-1}]$. Here, \mathbf{s}_k is the set of spectrum matched short sequences for the k th user. Find the matrix \mathbf{F} of filtered spreading sequences.
2. Calculate the maximum possible normalized interference I_k experienced by each user k given by $I_k = (\sum_{p=0, p \neq k}^{K-1} |R_{kp}|) / R_{kk}$.
 3. Find the maximum value of interference $I_{max} = \max(I_k)$ for all users.
 4. Repeat steps 1-3 Q times and pick the set of sequences which gives the minimum I_{max} .

Once the set of spreading sequences are found, we can assign these spreading sequences to the corresponding users so that the multiuser detector at the receiver can decode each user's information with considerably less performance degradation relative to their single user performance.

4. Long spreading codes with channel coding

In this subsection, we also consider the design of each user's spreading sequence where the knowledge of the rest of the users' spreading sequences is not necessary. Here, we attempt to maximize single user performance through the use of long spreading sequences or equivalently, by the use of different spreading sequences for different bits. The main advantage of this approach is that joint optimization of spreading sequences is not required since there is no attempt to minimize the short time cross correlation. This is useful in the situation where each user has the knowledge only on his frequency selective channel. Here, the average cross correlation between sequences (averaged over different bit intervals) can be made quite small since the length of the sequences is large. Although the average cross correlation is small, the instantaneous cross correlation can be quite large. Therefore, this approach is not suitable for

uncoded transmission as this will result in an error floor. However, in the presence of a channel code, the fact that instantaneous cross correlation can be large is not a significant issue due to the time diversity provided by the channel code.

B. Receiver structure

For the receiver at the base station, we use an MMSE receiver followed by a parallel interference canceller [18]. Here, the receiver includes a set of N matched filters, one for each user, followed by an MMSE receiver and an iterative interference rejection system. Each user's matched filter is matched to the filtered spreading sequence of the corresponding user. The output signal at the k th user's match filter is given by

$$z_{k,m} = \sum_{j=0}^{N-1} f_{k,j} r_{j,m}, \quad 0 \leq k \leq K-1. \quad (5.12)$$

The following iterative steps briefly describe the function of the MMSE front end-parallel interference cancellation detector.

1. Find the MMSE estimator of the k th user's information symbol as $\hat{x}_{k,m} = \sum_{p=0}^{K-1} A_{k,p} z_{p,m}$. Where $A_{k,p}$ is the k th row, p th column of \mathbf{A} which is given by $\mathbf{A} = [\mathbf{R} + \sigma^2 \mathbf{I}]^{-1}$.
2. Reconstruct the multiple access interference for each user k based on the estimation obtained in step 1. Let us assume that the calculated interference for the n th iteration, for the k th user is $I_{k,n}$.
3. For each user k , subtract the weighted multiple access interference given by $(I_{k,n} + I_{k,n-1})/2$ from the received signal \mathbf{r}_m . Here $I_{k,0} = 0$. This interference eliminated signal can be considered as the new input to the k th user's matched filter to get a more accurate decision for the k th user's bit $x_{k,m}$.

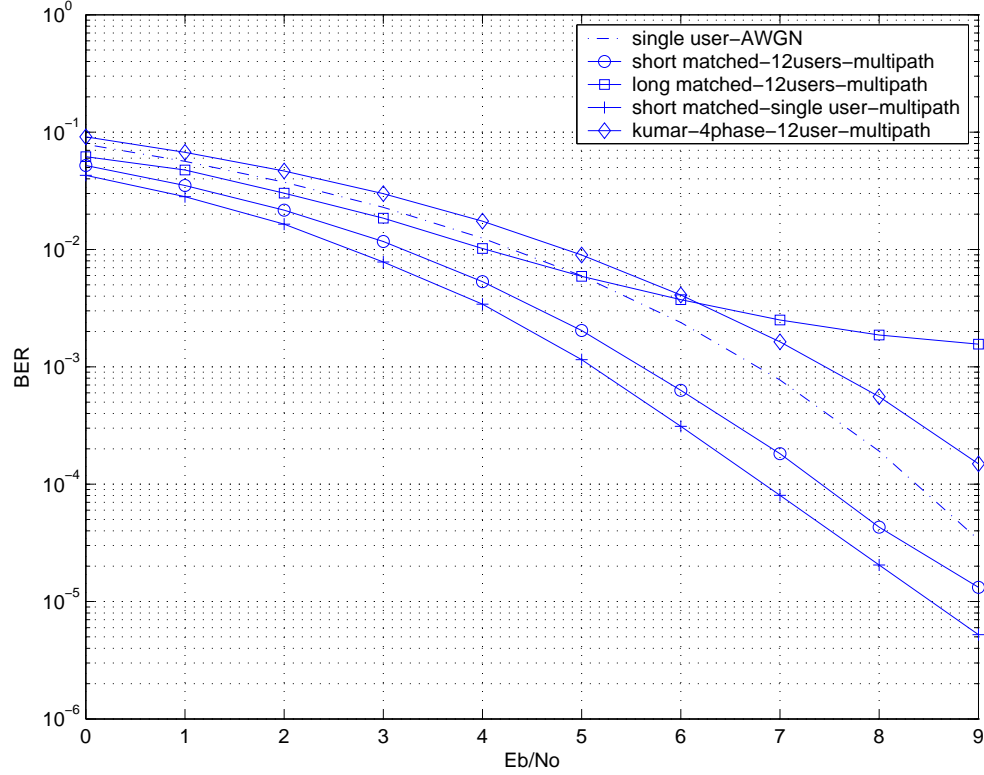


Fig. 21. BER performance comparison of the system with short codes. $N=16$, $K=12$.

4. Steps 2 and 3 are followed iteratively for a sufficient number of times until the BER of each user converges.

To verify the performance of the proposed method, simulations were carried out for the uplink of a DS-CDMA system. Each user's channel is assumed to be a 2-tap frequency selective slow fading channel, where taps are drawn from a Gaussian distribution and the power is normalized to one, which remains fixed for the period of transmission. A set of short spreading sequences are carefully selected according to the technique proposed in section A, subsection 3 and the receiver described in section B was used. To compare the performance of the proposed method, simulations were also carried out with 4-phase sequences proposed in [36] which are assigned

randomly to each user. Fig. 21 shows the performance of the designed short codes

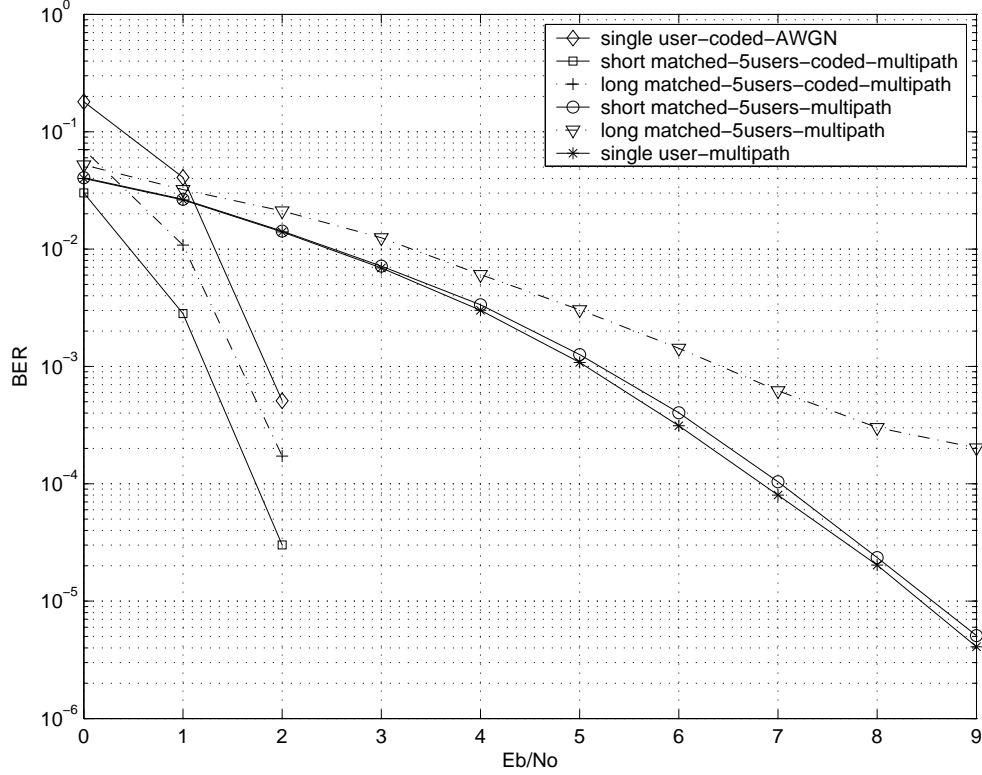


Fig. 22. BER performance comparison of the system with long codes [41]. $K=5$, $N=16$.

for a heavily loaded system with spreading code length 16. The number of users in this system is 12 corresponding to a 75% loading. Here the obtainable gain for spectrum matched sequences with the use of a sub optimal detector over single user performance in an AWGN channel is 1 dB at a BER of 10^{-3} . In this case, the spectrum matched spreading sequences give a 1.8 dB performance improvement over the 4-phase sequences proposed in [36]. We also have shown the performance of long spreading sequences (without optimizing the cross correlation). It can be seen from the figure that, the system with long spreading sequences results in an error floor

in the absence of channel codes. Furthermore, it can be noted that this is close to the optimized performance for uncoded BER in the range of 10^{-1} to 10^{-2} which is typically the region of interest in coded systems.

To demonstrate the effect of the use of a powerful channel code in the low SNR region, simulations were carried out with the use of a rate one-half turbo code where the generator polynomial of the component encoder is $[5,7]$ and the block length is 2000. As shown in Fig. 22, for a 5 user system with spreading length 16 with the use of channel coding, the error floor which occurred in an uncoded system can be eliminated. It is further shown that, by doing so, the performance of a coded system with long spreading codes is inferior to that of a coded system with short spreading codes only by about 0.5 dB. Furthermore, with the application of turbo codes BER performance of a system with long spreading codes is superior to the coded single user AWGN channel performance with turbo codes. Hence, it is clear that spectrally matched long codes along with a very powerful channel code can successfully be used in multipath CDMA systems. The BER performance of long codes is few tenths of a dB away from the performance of a system with spectrally matched short codes with good cross correlation properties.

CHAPTER VI

THE DESIGN OF SHAPING CODES FOR PARTIAL RESPONSE CHANNELS

In this chapter, we discuss the design of channel coding schemes for single-track/head and multi-track/head magnetic recording channels. The channel code is considered to be a concatenation of an inner shaping code and an outer channel code. The outer channel code is matched to the inner shaping code using the EXIT chart analysis. We mainly focus on the low-rate code design schemes. For this, we assume that the magnetic recording channel as a frequency selective channel and try to design the optimum shaping codes by assuming that the shaping codes are the spreading sequences in an equivalent multiuser frequency selective system. It is important to note that the inputs to the magnetic recording channels are derived from a binary alphabet. Hence, we design the spreading sequences with binary chips. We show that our proposed algorithm in Chapter IV to design finite alphabet spreading sequences for frequency selective channel can successfully be used to design above shaping sequences for magnetic recording channels.

For single-track magnetic recording channels, we design the shaping sequences such that the trellis corresponding to the shaping code has multiple parallel branches to increase the rate of the outer code which will also increase the overall rate of the concatenated code. For multi-track recording schemes, we design the inner shaping sequences with a low rate. These shaping sequences for the tracks are designed jointly to maximize the single-track performance at the low rate region, while minimizing the interference from the neighboring tracks. The encoding is performed separately and decoding is performed jointly at the decoder. Performance of multi-track recording schemes with the use of per-survivor decoding is also discussed.

A. Background

Channel coding is necessary for digital magnetic recording for a variety of reasons such as error correction, timing recovery and the reduction of the effect of nonlinearities. The channel codes should be selected such that they are easily implementable with a considerably small penalty on the information density. The design of channel codes for partial response channels has recently received some attention. According to information theory, the capacity of a power-constrained partial response channel whose input alphabet is not constrained to be finite can be obtained by the well known waterfilling argument [42]. However, in a magnetic recording channel, data is encoded in the media by magnetizing the magnetic domains in one of the two possible directions (longitudinal/perpendicular). Hence, the input alphabet is constrained to a binary one.

A partial response channel with constrained input alphabet can be represented by a finite state machine and the definition of the capacity C of a partial response channel is described in [43]. It should be noted that, there are no known analytical result for either the capacity or the spectrum of the input distribution for constrained input alphabets as in the unconstrained input alphabet case. The i.u.d capacity $C_{i.u.d}$ of a partial response channel refers to the information rate when inputs are independent and uniformly distributed (i.u.d.) random variables.

The computation of the capacity C and the i.u.d. capacity $C_{i.u.d}$ of a partial response channel has been a subject of researchers' attention for some time. In [44], Goldsmith and Varaiya have formulated the information rate of a finite-state machine channel. This formulation was generalized for ISI channel by Sharma and Singh in [45]. They have also computed a lower bound on the channel capacity of partial response channels. Arnold and Loeliger [46] and Pfister et al. [47] proposed a Monte

Carlo method to compute the information rate of a finite-state machine channel where the inputs are generated from a Markov process. They have also computed a lower bound for the i.u.d. capacity on C . In [48], Kavcic et. al. have proposed a method to design capacity-approaching codes for partial response channels. Here, the codes are constructed as concatenations of inner trellis codes and outer low density parity check (LDPC) codes. In the design, the inner trellis code is constructed to mimic the transition probabilities of a first order Markov process that achieves a high information rate. The outer LDPC code is optimized using the density evolution. However, this scheme has high computational complexity even for the channels with short memories.

In modern hard disks, multiple heads are used for fast recoding of data to the magnetic disk and retrieval of data from it. Since magnetic recording tracks have become narrower and narrower to obtain a great increase in the areal density, the read-back signals of the heads inevitably interfere with each other causing inter-track interference. Hence, a magnetic recording track can be modelled as a partial response channel that interferes only with adjacent tracks called the inter-track interference (ITI). For example, in a disk configuration where only N tracks are written and read at a time, the inter-track interference matrix can be represented as

$$\mathbf{H} = \begin{bmatrix} 1 & 0 & 0 & 0 & \dots & 0 \\ \alpha & 1 & \alpha & 0 & \dots & 0 \\ 0 & \alpha & 1 & \alpha & \dots & 0 \\ \vdots & \vdots & \vdots & \vdots & \vdots & \vdots \\ 0 & \dots & \dots & \dots & \dots & 1 \end{bmatrix}.$$

where α is the inter-track interference.

In [49] and [50], the general problem of simultaneous detection of multiple tracks using multiple heads was studied. In [49], a maximum likelihood detection that

operates on the samples of the zero forcing equalizer is proposed. In [50], the detection is based on decision feedback equalizing and a simple algorithm for computing the performance of an infinite-length decision feedback equalizer is presented.

This chapter focusses on two areas. First, we discuss the design of inner shaping codes for single-track/head magnetic recording schemes. The inner shaping code is a trellis code and the shaping trellis has multiple parallel branches to increase the rate of the outer code. The design of shaping codes with a high rate also increases the overall rate of the concatenated code. For a dicode channel, our proposed scheme with rate $2/3$ outer shaping code outperforms the scheme with bi-phase coding as shaping codes. Secondly, for multi-track recoding schemes, we design the inner shaping sequences with a low rate. These shaping sequences for the tracks are designed jointly to maximize the single-track rate at low rate region, while minimizing the interference from the neighboring tracks. The encoding is performed separately for different tracks and for each track, the outer channel code is matched to the inner shaping code using EXIT chart analysis. The decoding is performed jointly at the decoder. We also show that the performance of multi-track recoding schemes with the use of per-survivor decoding is very close to the optimum joint decoding when the shaping sequences are designed jointly.

B. The design of shaping codes for single-track magnetic recording systems

As described in [51], at low SNR region, the channel output is mainly contributed by AWGN noise. Hence, the technique for unconstrained input signals can be used as a guideline to design the codes with constrained alphabets. Further, it was shown in [51] that, at the low rate region, due to the very low input energy, most of the power of the waterfilling spectrum is constrained at the bottom of the inverted channel. Hence,

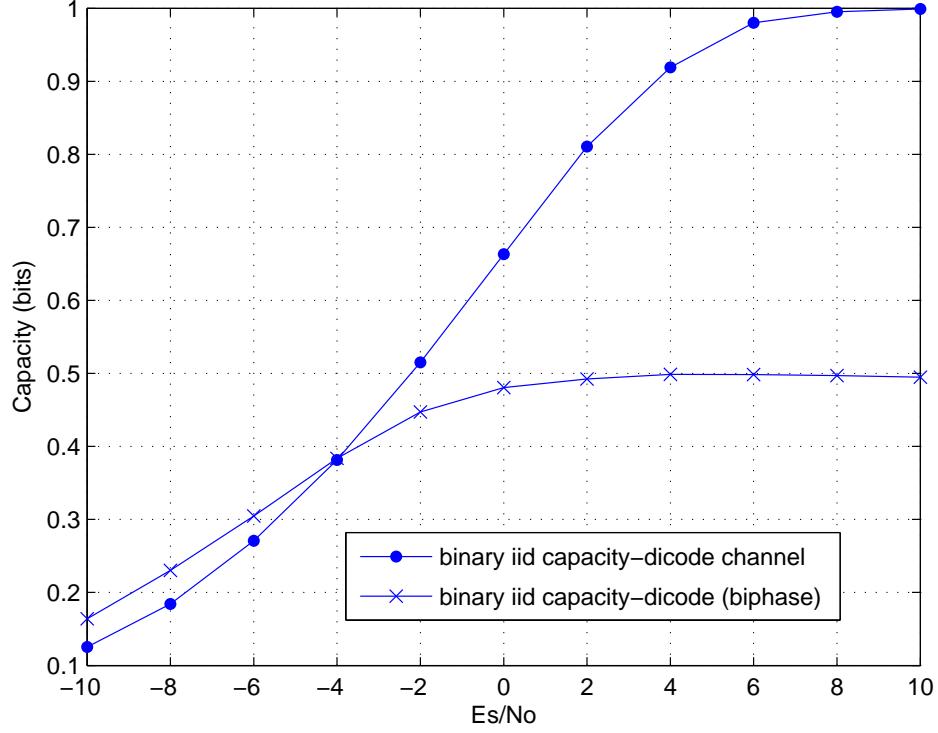


Fig. 23. i.u.d. capacity dicode channel with bi-phase coding vs i.u.d. capacity of dicode channel.

in the low rate region, the waterfilling spectrum of a channel code corresponds to the maximization of the energy of the code at the channel output. Fig. 23 shows the i.u.d. capacity and the capacity of the channel for a dicode channel $(1 - D)$ with bi-phase coding [51]. The bi-phase code can be represented as a two-state trellis with two branches emerging from each state with input sequences $[0 \ 1]$ and $[1 \ 0]$. The figure clearly shows that, at the low rate region of channel capacity less than 0.4 bits/sample, the capacity of the system with bi-phase codes outperforms the i.u.d. capacity of the channel with binary inputs. The main disadvantage of the above scheme is that, there is a reasonable rate loss in the high SNR region. The maximum

achievable rate is 0.5 bits/sample where the i.u.d capacity and the capacity of the channel can reach up to 1 bits/sample.

As we have mentioned in the previous paragraph, with the use of shaping codes that form the shaping trellis with no parallel branches, the maximum achievable rate is 0.5 bits/sample. One option to increase the overall rate of the system is to design the shaping codes that form a trellis with parallel branches. For example, if the shaping code length is n and the number branches from each state is k , then the achievable rate is k/n . The important consideration here is that, these shaping codes for each branch has to be carefully selected so that the spectrum of the code closely follows the waterfilling spectrum. Note that, at low rate region, waterfilling spectrum is equivalent to the spectrum that maximizes the energy of the shaping code at the output of the channel.

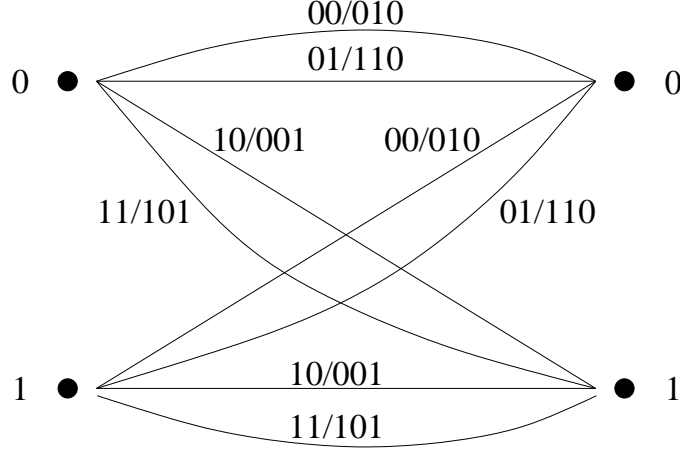


Fig. 24. Trellis section with assigned shaping codes.

The design algorithm for shaping codes can be described as follows. We consider a DS-CDMA system with $2^k/2$ number of users. Users' spreading sequences' length is n . Each user's channel is assumed to be a frequency selective channel with channel

response $1 - D$. Based on the iterative algorithm proposed in section A, Chapter IV, we design the shaping codes for the frequency selective multiuser system. But, in each user's iteration, the sequences are mapped onto binary sequences rather than onto unit circle sequences using the Lagrangian relaxation method. It should be noted that the algorithm tries to generate the sequences whose filtered versions are orthogonal. But, we know that, the inverted version of the sequences, which are not generated by the algorithm, can also be used as shaping sequences since our focus here is to generate the shaping sequences with higher minimum distance and desired spectra. Altogether there will be 2^k number of nearly bi-orthogonal sequences and we can assign those sequences as for the branches of the trellis. To illustrate the

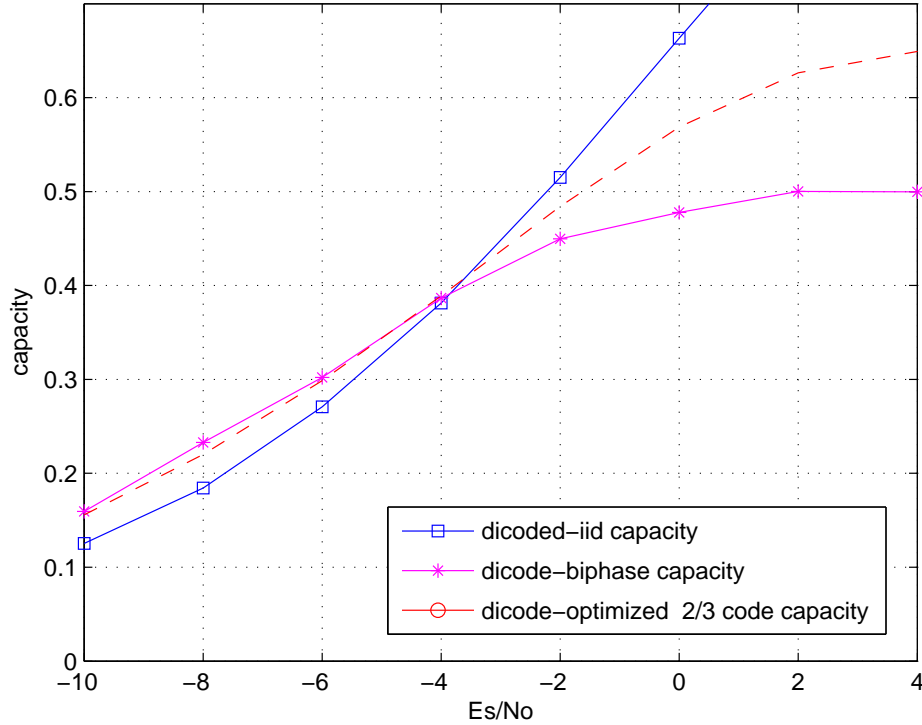


Fig. 25. Capacity of the scheme with parallel branches. Rate=2/3.

above shaping codes assigning algorithm, we have used shaping codes with length 3 for a dicode channel with 2 parallel branches. Here, each state transition is defined by one of the four possible two bit input sequences as shown in Fig. 24. Hence, the maximum overall rate is $2/3$ bits/sample. The channel capacity of the scheme with assigned shaping codes is shown in figure Fig. 25. The channel capacity is calculated using the Monte-Carlo simulation method proposed in [46]. It can be seen that, at low rates, the $2/3$ shaping code gives almost the same capacity as that of the bi-phase code. At higher rates around 0.5 bits/sample, the $2/3$ shaping codes perform better than the bi-phase code and the capacity gap between i.u.d. input sequences and the proposed shaping code is significantly small. Hence, our proposed coding scheme is a better option for a wide range of code rates.

C. The design of shaping codes for a multi-track magnetic recording systems

As we have discussed earlier, in a multi-track recording system, there are more than one magnetic read/write heads hovering over the magnetic disk/tape which allow reading or writing multiple tracks simultaneously allowing fast retrieval and recording of information. If the inter-track gap is reasonably large then we can assume that there are no inter-track interference and we can consider the tracks as a set of parallel channels. However, in practice, track widths are made to be smaller and tracks are aligned closely to increase the recording density. This inevitably causes inter-track interference. In this subsection, we discuss the method of designing of low rate inner shaping codes and outer channel codes for a two-track magnetic recoding media.

1. The design of shaping codes for two-track magnetic recording systems

Let $x_1(D)$ and $x_2(D)$ be D transforms of constrained input sequences $[x_{11}, x_{12}, x_{13} \dots]$ and $[x_{21}, x_{22}, x_{23} \dots]$ that are going to be recorded on a two-track magnetic recording channel. Let the channel inter-track interference be α . Then, the channel correlation matrix is given by

$$\mathbf{H} = \begin{bmatrix} 1 & \alpha \\ \alpha & 1 \end{bmatrix}.$$

If the recoded signals on tracks are given by $y_1(D)$ and $y_2(D)$ then, $y_1(D) = (x_1(D) + \alpha x_2(D))h(D) + n_1(D)$ and $y_2(D) = (x_2(D) + \alpha x_1(D))h(D) + n_2(D)$. Here, $h(D)$ is the D transform of the channel impulse response. If we simply combine $y_1(D)$ and $y_2(D)$ we get a channel of

$$\mathbf{y}(D) = (1 + \alpha)(x_1(D) + x_2(D))h(D) + n(D). \quad (6.1)$$

where $n(D) = n_1(D) + n_2(D)$.

The optimum way of detecting $x_1(D)$ and $x_2(D)$ is the maximum likelihood detection. Obviously the detection of $x_1(D)$ and $x_2(D)$ from $y(D)$, hereinafter the combined decoding, causes some capacity loss over the detection of $x_1(D)$ and $x_2(D)$ from $[y_1(D) \ y_2(D)]$, hereinafter the joint decoding. In Appendix A, we have derived the fractional capacity loss due to the combined detection scheme over the joint detection scheme. Fig. 26 shows the fractional capacity loss of the combined detection scheme with respect to the achievable capacity due to the joint detection scheme at the low rate region. According to the figure, we can see that, when the inter-track interference α is greater than 0.6, the fractional capacity loss is less than 5% of the capacity due to the joint detection. Hence, this combined model can be used when we have very heavy inter-track interference. Here after, for two track channel, we

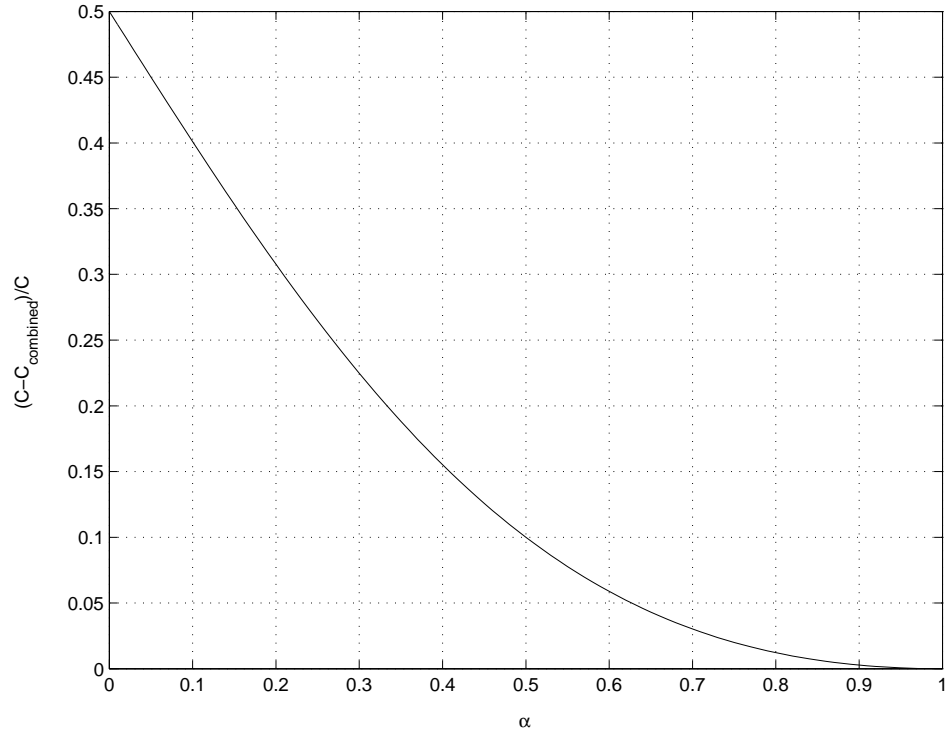


Fig. 26. Fractional capacity loss due to the combining of two channels.

assume the model proposed in (6.1). That is, at the decoder, we can simply combine the received signals $y_1(D)$ and $y_2(D)$ and perform the decoding assuming the received signal is $y(D)$. In other words, the decoding problem becomes a multiuser detection problem in a frequency selective channel. In a multiuser system, the optimal way of designing users' codes is to design them such that the codes follow the multiuser waterfilling spectrum. However, at low rate region with identical channels, multiuser waterfilling spectrum lies at the bottom of the common inverted channel and each user's spectrum would be such that they try to maximize the single user performance. Fig. 27 shows the EXIT chart for a two-track magnetic recording system where the channel frequency responses of the tracks overlap (both of the channels' impulse response is $1 - D$). A heavy inter-track interference ($\alpha > 0.6$) is assumed hence the

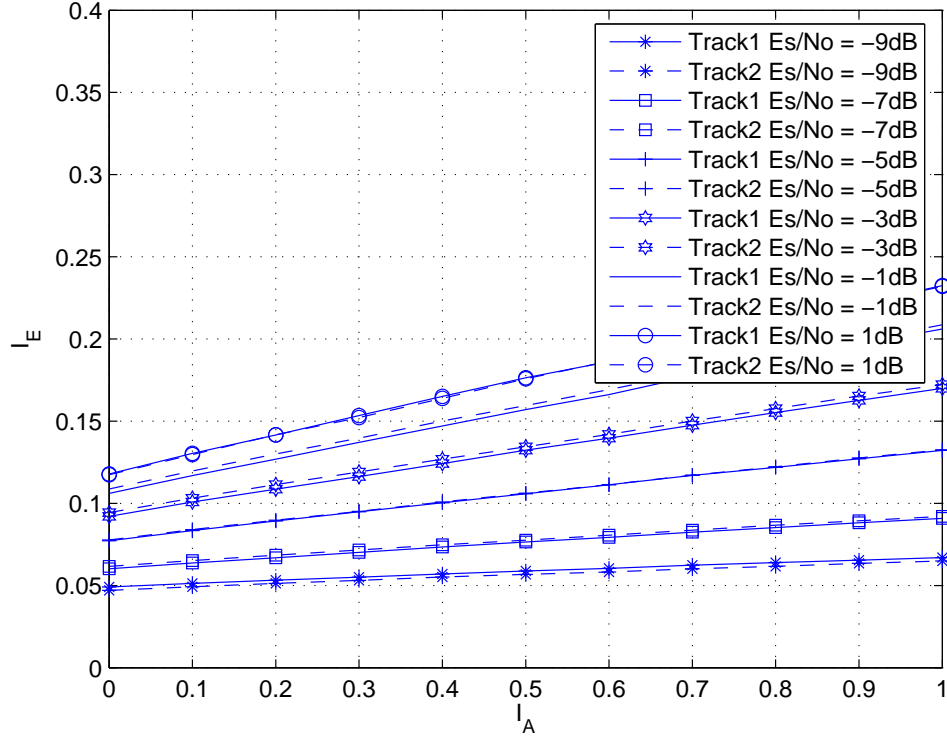


Fig. 27. The EXIT chart for the two-track magnetic recording channel with individually optimized sequences. Optimum combined decoding assumed. Inner code rate is 0.25 bits/sample.

combined model is applicable. The shaping codes, with a rate of 0.25 bits/sample, are such that 1 is mapped to [0101] and 0 is mapped to [1010]. In this case, we can see from the figure that the EXIT charts for the channels are no longer flat. Hence, if we use an outer code that is optimized for an AWGN channel, there will be a rate loss or else the decoder should iterate number of times between the outer decoder and inner decoder.

The reason behind the above impairment is that, the codes we have designed are matched only to the waterfilling spectrum of the channels. The cross correlation effect

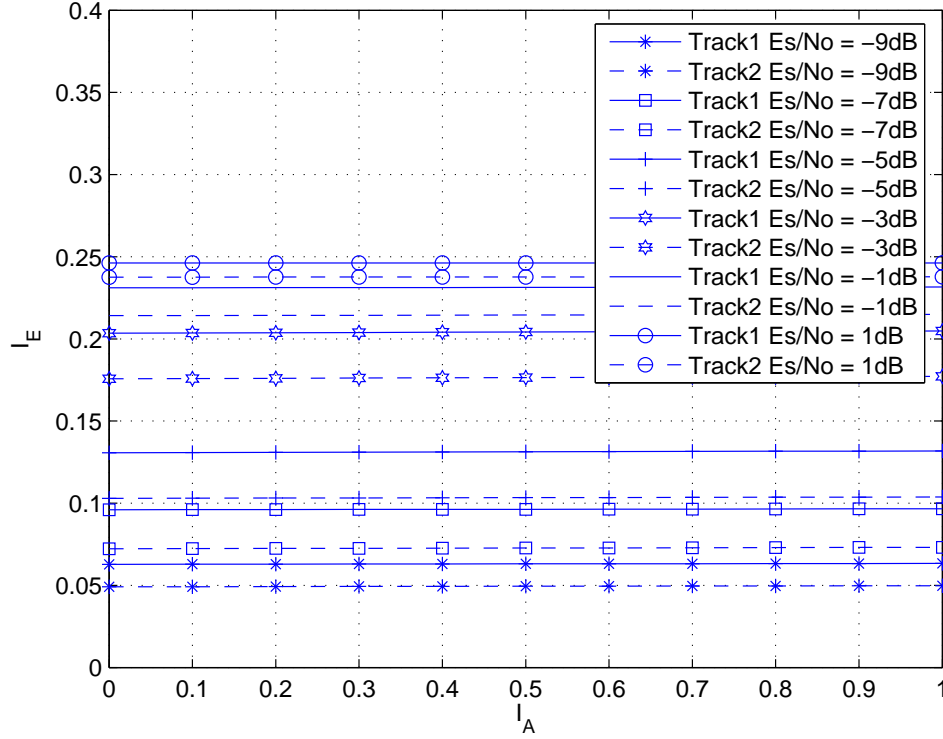


Fig. 28. The EXIT chart for two-track channel with jointly optimized sequences. Optimum combined decoding is assumed. Inner code rate is 0.25 b/sample.

among the shaping sequences of two different tracks were not taken in to consideration. In contrast to the above results, we will soon show that if we design the tracks' shaping codes jointly, we can achieve better rates for the two-track recording channel while using outer codes which are optimized for AWGN channels. For this, the design technique is as follows. Let's assume that for each track's shaping trellis, there are P outgoing branches and there are K number of tracks in the system and the shaping code length is L .

1. Assume a DS-CDMA system with $PK/2$ users having the same ISI channel with spreading length L .

2. Optimize the sequences of $PK/2$ users according to the algorithm proposed in section A, Chapter IV to get a set of binary spreading sequences. It should be noted that the algorithm proposed in section A, Chapter IV produces nearly orthogonal sequences.
3. Assign $P/2$ sequences for each track. The rest of the $P/2$ branches are obtained by inverting the assigned $P/2$ sequences.
4. For each track's channel trellis, we can consider the total P sequences as branches emerging from the states.

For example, let's consider a two-track dicode channel with 4 bit shaping codes. Here, each state has two outgoing branches corresponding to input bits 0/1. Then, the number of codes to be optimized is $2 \times 2 = 4$. Since we can use both shaping codes and their inverted sequences, the required number of length 4 sequences to be optimized is 2. Fig. 28 shows the EXIT chart obtained by optimizing the sequences according to the earlier mentioned algorithm. The optimized sequences for the first channel are given by $[1, 0, 1, 0]$ and $[0, 1, 0, 1]$ and the optimized sequences for the second channel are given by $[0, 1, 1, 0]$ and $[1, 0, 0, 1]$. We can clearly see that the EXIT charts are flat hence it is possible to use outer codes which are optimized for AWGN channels. Further, we can see that the achievable sum rate is higher than that of the individually optimized sequences. This can be seen from Fig. 29 too. That is, there is a sum rate gain when we optimize the tracks' shaping codes jointly over the individually matched codes.

D. Two-track system with suboptimal decoding

In the previous subsection, the EXIT chart analysis and the capacity calculations assumed that the receiver performs the optimum decoding. The maximum Likelihood

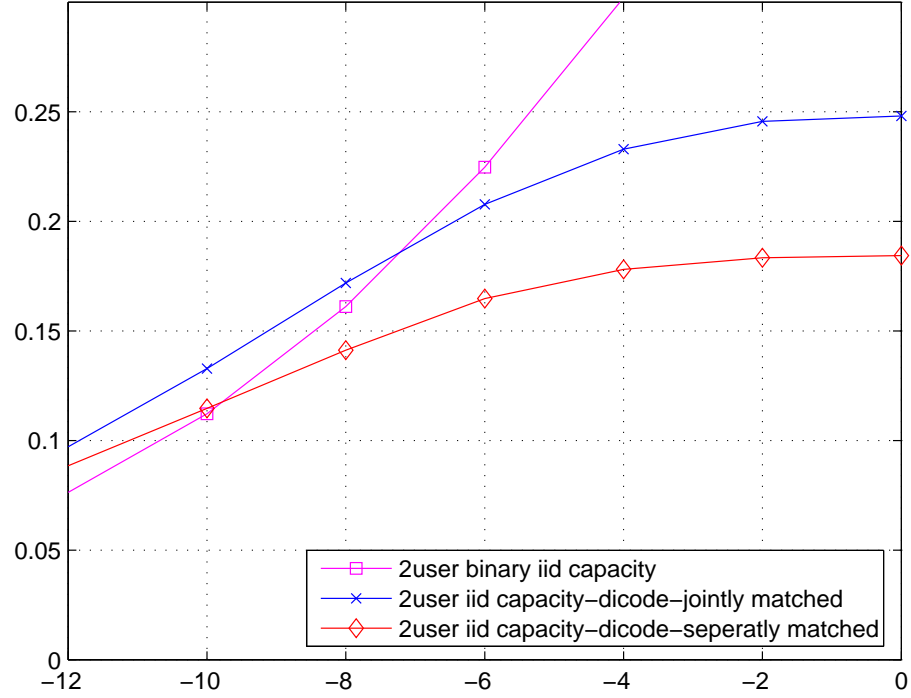


Fig. 29. Per-user channel capacity for different shaping codes. Each track's channel is $1 - D$.

Sequence Estimation is the optimum decoder for a data sequence that has transmitted over a dispersive and noisy channel. But, for a multiuser/multi-track system, since the number of states in the joint MLSE decoder increases exponentially with the number of users/tracks and the the length of the channel impulse response, a high-complexity trellis decoder is required which is prohibitively complex. In [52], Raheli proposed a suboptimal alternative to this classical technique and it is called the per-survivor decoding technique. The basic idea behind the per-survivor decoding is to cancel the effects of residual ISI from the interfering user directly within the calculation of each transition metric in the trellis based on the data sequence associated with the

survivor leading to that transition.

Here, we describe the suboptimum per-survivor decoding algorithm. Let the m th state of the k th track's channel trellis at t th time interval is given by m_t^k . Then, any branch in the trellis can be represented as $b_t(m_t^k, m_{t+1}'^k)$. Let the input sequence and the corresponding output sequence related to the trellis branch $b_t(m_t^k, m_{t+1}'^k)$ is given by $x_t(m_t^k, m_{t+1}'^k)$ and $y_t(m_t^k, m_{t+1}'^k)$ respectively. Further, we assume that y_t is the noisy received sequence at time t . Note that, at the beginning, both tracks' channels are flushed with zeros to start at the zeroth state $m_0^k = 0$.

The suboptimal decoding algorithm is as follows.

FOR $t=0:\text{length_of_the_trellis}$

1. For each branch $b_t(m_t^1, m_{t+1}'^1)$ of the track 1 trellis, calculate $y_t^1 = y_t(m_t^1, m_{t+1}'^1)$. Subtract y_t^1 from y_t to form $y_t - y_t^1$. For the track 2, estimate $y_t^2(m_t^2, m_{t+1}'^2)$ based on the minimum Euclidean distance.
2. For each branch $b_t(m_t^1, m_{t+1}'^1)$ for the track 1 trellis, find the branch matrix $\gamma_t(m_t^1, m_{t+1}'^1)$. Here, the estimated $y_t^2(m_t^2, m_{t+1}'^2)$ in step 1 is used to calculate $\gamma_t(m_t^1, m_{t+1}'^1)$.
3. At time $t + 1$, at each state of trellis $m_{t+1}'^1$, calculate the survivor path. From the survivor path calculate the state of the track 2 trellis $m_{t+1}'^2$

END

If the modulation index is M and the memory of the channel is L , there is total number of $M^2 2^L + 2M 2^L$ computations to find the branch matrices of both the track' channel trellises. Hence, the computational complexity of the per-survivor decoding scheme is $\frac{M^2 2^L + 2M 2^L}{M^2 2^{2L}} = (1 + \frac{2}{M}) \frac{1}{2^L}$ th of the optimal joint decoding scheme.

E. Simulation results

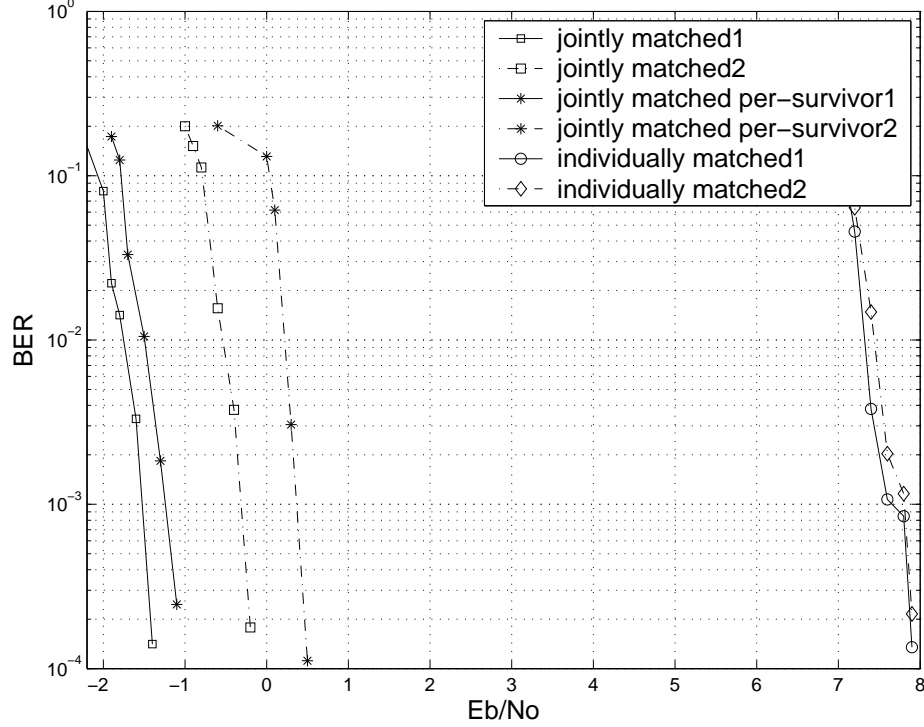


Fig. 30. BER performance with different shaping codes. $N=40,000$, overall rate is 0.125. Rate LDPC=0.50.

Fig. 30 shows the BER performance of different inner shaping codes. Inner shaping codes with code rate 0.25 are selected to match the channels' power spectra. The outer code is an irregular LDPC code of rate 0.50 optimized for an AWGN channel. A degree profile of maximum left degree 100 and right degree 12 is selected. The overall rate of the combined outer LDPC and inner shaping code is 0.125. We consider two cases. In the first case, we design each tracks's shaping codes disregarding other tracks' presence (greedy algorithm). In the second case, we optimize tracks' shaping codes jointly using the optimization algorithm discussed in the previous subsection.

For individually matched shaping codes, for both tracks, we have used the [1010]

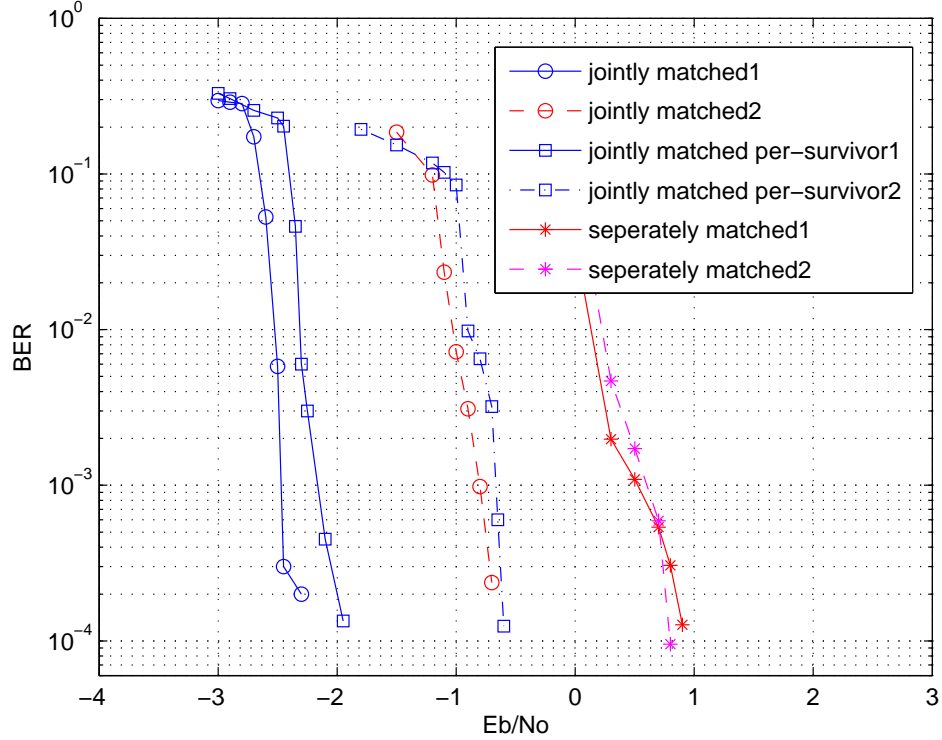


Fig. 31. BER performance with different shaping codes. $N=40,000$, overall rate is 0.0625. Rate LDPC=0.25.

shaping code and its inverted sequence [0101] as shaping sequences. For jointly optimized codes, we have used our proposed algorithm to obtain the set of shaping sequences. The corresponding rate 0.25 shaping codes obtained from the optimization scheme are [1010] and its inverted sequence for the first channel and, [0110] and its inverted sequence for the second channel.

It can be seen from the figure that, with jointly matched shaping codes, we can achieve an 8 dB SNR gain than that of using individually matched shaping codes. We have also simulated the performance of the system with the per-survivor decoding scheme. It should be noted that, for the per-survivor decoding scheme, in step 1 of

the decoding algorithm, to estimate $y_t^2(m_t^2, m_{t+1}^{'2})$, we simply despread $y_t - y_t^1$. It can be proved that, there is a 25% decrease in the computational complexity in the per-survivor decoding scheme over the optimal decoding scheme. The performance of the suboptimal per-survivor decoding scheme is about 0.50 dB inferior to that of the optimal joint decoding scheme. Since the suboptimal per-survivor decoding scheme uses decision feedback, we should first decode the track whose shaping codes has the highest filtered energy. In our example, it can be easily observed that the first track's shaping sequence has the highest filtered energy. We have also separated tracks by simply despreading. It is found that the performance of this scheme only around 0.3 dB away from that of the per-survivor decoding scheme. However, for the scheme where despreading is used to separate the tracks, the computational complexity is just over 50% of the computational complexity of the optimal joint decoding scheme.

Fig. 31 shows that, when we use an LDPC code of rate 0.25 (overall rate of 0.0625 bits/sample), the performance loss due to the use of individually shaped sequences is not that severe. But, still it is possible to get a 2 dB gain by designing the multi-track' shaping sequences jointly.

From the above observations we can conclude that, at the low rate region, when the magnetic tracks have overlapping spectra with high ITI, individually designed shaping sequences degrades the system performance and the joint designing of shaping sequences is a better option.

CHAPTER VII

CONCLUSIONS

In this dissertation, we have proposed some novel techniques to design the spreading/shaping sequences for frequency selective multiuser systems. These spreading/shaping sequences are designed assuming that the designed unit, which can be either the transmitter or the receiver, has access to the channel state information. The interesting observation uncovered in the dissertation is that, irrespective of the constellation of the chips of the spreading sequences, the users in the system optimize their performance by restricting the spectrum of each user's sequence to a narrow frequency band at the spectral peaks of that user's channel.

In Chapter I, we have given an introduction to the design of constrained and unconstrained amplitude spreading/shaping sequences. In Chapter II, the underlined theoretical background which was necessary to develop the spreading/shaping sequence design schemes was presented.

In Chapter III, we have approached the problem of designing of spreading sequences in frequency domain perspective. Based on the frequency domain characteristics of the spreading sequences with unconstrained amplitudes and phases we have proposed a reduced-rank sequence design algorithm. The proposed scheme helps to reduce the computational complexity and the feedback bandwidth. The selection of the subspace for the basis vectors based on the frequency selectivity of a channel also allows us to improve the performance of some existing sequence design algorithm proposed for frequency selective channels.

In Chapter IV, the design of constrained amplitude spreading sequences for frequency selective channels was discussed. To design those constrained amplitude sequences, different approaches were taken. For this, we have used the frequency domain

characteristics of the unconstrained spreading sequences to find a set of constrained amplitude set of sequences for a given set of channel. This was done either by carefully assigning already existing set of sequences for given set of users or by mapping constrained amplitude sequences onto a unit circle.

In Chapter V, we have proposed an approach to design each user's spreading sequence that follows a specific power spectrum. In this case, first we have assumed a long chip sequence generated from an output of a first order Markov chain where the entries of the transition probability matrix were selected such that the power spectrum of each user's chip sequence closely follows the user's desired spectrum. Once the long spreading sequence is generated, a set of short spreading sequences which closely follow the user's desired spectrum is obtained. Once a set of single user spreading sequences are designed for each user's channel we select the optimum set, one code from each user, such that the cross correlation among the users' spreading sequences are minimized.

In Chapter VI, the design of shaping codes for single-head and multi-head magnetic recoding channels was discussed. The shaping sequences were designed assuming that the branch symbols of the shaping trellises were short spreading codes matched to the magnetic recoding channels. The outer channel code was matched to the inner shaping code using the EXIT chart analysis. For multi-track recoding schemes, encoding was performed separately and decoding was performed jointly at the decoder. Performance of multi-track recoding schemes with the use of per-survivor decoding was also discussed.

REFERENCES

- [1] L. R. Welch, "Lower bounds on the maximum cross correlation of signals," *IEEE Transactions on Information Theory*, vol. 3, no. 20, pp. 397-399, May 1974.
- [2] M. Rupf and J. L. Massey, "Optimum sequence multisets for synchronous code-division multiple-access channels," *IEEE Transactions on Information Theory*, vol. 40, no. 4, pp. 1261-1266, July 1994.
- [3] P. Viswanath, V. Anantharam and D. N. C. Tse, "Optimal sequences, power control, and user capacity of synchronous CDMA systems with linear MMSE multiuser receivers," *IEEE Transactions on Information Theory*, vol. 45, no. 6, pp. 1968-1983, September 1999.
- [4] S. Ulukus and R. D. Yates, "Iterative construction of optimum signature sequence sets in synchronous CDMA systems," *IEEE Transactions on Information Theory*, vol. 47, no. 5, pp. 1989-1998, July 2001.
- [5] G. S. Rajappan and M. L. Honig, "Multi-dimensional amplitude control for DS-CDMA Rajappan," in *Vehicular Technology Conference*, vol. 2, pp. 1256-1260, May 1999.
- [6] T. F. Wong and T. M. Lok, "Transmitter adaptation in multicode DS-CDMA systems," *IEEE Journal on Selected Areas in Communications*, vol. 19, no. 1, pp. 69-82, January 2001.
- [7] T. F. Wong and T. M. Lok, "Spreading sequence adaptation in multicode CDMA systems," in *IEEE International Conference on Communications*, vol. 3, pp. 1375-1379, June 2000.

- [8] W. M. Jang, B. R. Vojcic, and R. L. Pickholtz, "Joint transmitter-receiver optimization in synchronous multiuser communications over multipath channels," *IEEE Transactions on Communications*, vol. 46, no. 2, pp. 269-278, February 1998.
- [9] G. S. Rajappan and M. L. Honig, "Spreading code adaptation for DS-CDMA with multipath," in *IEEE Milcom*, vol. 2, pp. 1164-1168, 2000.
- [10] J. I. Concha and S. Ulukus, "Optimization of CDMA signature sequences in multipath channels," in *Proceedings of IEEE Vehicular Technology Conference*, pp. 1978-1982, Spring 2001.
- [11] D. C. Popescu and C. Rose, "Interference avoidance applied to multiaccess dispersive channels," in *Thirty-Fifth Asilomar Conference on Signals, Systems and Computers*, vol. 2, pp. 1200-1204, November 2001.
- [12] V. Krishnamurthy, X. Wang and G. Yin, "Adaptive spreading code optimization in multi-antenna multipath fading channels in CDMA," *IEEE International Conference on Communication*, vol. 4, pp. 2445-2449, May 2003.
- [13] V. Krishnamurthy, X. Wang and G. Yin, "Spreading code optimization and adaptation in CDMA via discrete stochastic approximation," *IEEE Transactions on Information Theory*, vol. 50, no. 9, pp. 1927-1949, September 2004 .
- [14] E. D. Daniel, C. D. Mee and M. H. Clark, *Magnetic Recording: The First 100 Years*, New York: Wiley-IEEE Press, 1998.
- [15] E. Soljani and C. N. Georgiades, "On coding in multi-track, multi-head, disk recording systems," in *IEEE Global Telecommunications Conference*, vol. 4, pp. 18-22, December 1993.

- [16] S. Verdu, *Multiuser Detection*, New York: Cambridge University Press, 1998.
- [17] P. Patel and J. Holtzman, "Analysis of a simple successive interference cancellation scheme in DS/CDMA system," *IEEE Journal on Selected Areas of Communications*, vol. 12, pp. 796-807, June 1994.
- [18] D. Divsalar, M. K. Simon, and D. Raphaeli, "Improved parallel interference cancellation for CDMA," *IEEE Transactions on Communications*, vol. 46, no. 2, pp. 258-268, February 1998.
- [19] C. Berrou, A. Glavieux, and P. Thitimajshima, "Near Shannon limit error-correcting coding and decoding: Turbo codes," in *Proceedings of International Conference on Communications*, pp. 1064-1070, 1993.
- [20] S. Benedetto and G. Montorsi, "Unveiling turbo codes: Some results on parallel concatenated coding schemes," *IEEE Transactions on Information Theory*, pp. 409-428, vol. 42, no. 2, March 1996.
- [21] L. Bahl, J. Cocke, F. Jelinek, and J. Raviv, "Decoding of linear codes for minimizing symbol error rate," *IEEE Transactions on Information Theory*, vol. 20, no. 2, pp. 284-287, March 1974.
- [22] R. G. Gallager, "Low-density parity-check codes," *IRE Transactions on Information Theory*, vol. 8, pp. 21-28, January 1962.
- [23] D. J. C. MacKay and R. M. Neal, "Near Shannon limit performance of low density parity check codes," *IEEE Electronics Letters*, vol. 32, no. 18, pp. 1645-1655, August 1996.
- [24] R. M. Tanner, "A recursive approach to low complexity codes," *IEEE Transactions on Information Theory*, vol. 27, pp. 533-547, September 1981.

- [25] W. E. Ryan, *CRC Handbook for Coding and Signal Processing for Recoding Systems*, New York: CRC Press, 2004.
- [26] R. G. Gallager, *Low-Density Parity-Check Codes*, Cambridge, MA: M.I.T. Press, 1963.
- [27] S. ten Brink, "Convergence behavior of iteratively decoded parallel concatenated codes," *IEEE Transactions on Communications*, vol. 49, no. 10, pp. 1727-1737, October 2001.
- [28] A. Ashikhmin, G. Kramer and S. ten Brink, "Extrinsic information transfer functions: Model and erasure channel properties," *IEEE Transactions on Information Theory*, vol. 50, no. 11, pp. 2657-2673, November 2004.
- [29] D. Bertsekas, *Nonlinear Programming*, Belmont, MA: Athena Scientific, 2000.
- [30] Roger A. Horn and Charles R. Johnson, *Matrix Analysis*, New York: Cambridge University Press, 1999.
- [31] T. K. Moon and W. C. Stirling, *Mathematical Methods and Algorithms for Signal Processing*, New Jersey: Prentice Hall, 2000.
- [32] G. S. Rajappan and M. L. Honig, "Signature sequence adaptation for DS-CDMA with multipath," *IEEE Journal on Selected Areas in Communications*, vol. 20, no. 2, pp. 384-395, February 2002.
- [33] B. J. Peiris, K. R. Narayanan and S. L. Miller, "A frequency domain approach to designing a set of spreading sequences in DS-CDMA systems with frequency selective fading," *IEEE Transactions on Wireless Communication*, vol. 5, no. 9, pp. 2386-2395, September 2006.

- [34] G. S. Golub and C. F. V Loan, *Matrix Computations*, Baltimore: The John Hopkins University Press, 1996.
- [35] S. Boyd and L. Vandenberghe, *Convex Optimization*, Cambridge: Cambridge University Press, 2004.
- [36] S. Bostaz, R. Hammons and P. Y. Kumar, "4-phase sequences with near optimum correlation properties," *IEEE Transactions on Information Theory*, vol. 38, no. 3, pp. 1101-1113, May 1992.
- [37] J. Oppermann and B. S. Vucetic, "Complex spreading sequences with a wide range of correlation properties," *IEEE Transactions on Communications*, vol. 45, no. 3, pp. 365-375, March 1997.
- [38] R. S. Cheng and S. Verdu, "Gaussian multiaccess channels with ISI: Capacity region and multiuser water-filling," *IEEE Transactions on Information Theory*, vol. 5, no. 3, pp. 773-785, May 1993.
- [39] W. Yu, W. Rhee, S. Boyd and J. M. Cioffi, "Iterative water-filling for Gaussian vector multiple access channels," in *IEEE International Symposium on Information Theory*, pp. 322-322, 2001.
- [40] W. Hirt and J. L. Massey, "Capacity of the discrete-time Gaussian channel with intersymbol interference," *IEEE Transactions on Information Theory*, vol. 34, no. 3, pp. 380-388, May 1998.
- [41] B. J. Peiris, K. R. Narayanan and S. L. Miller, "A technique to design spreading sequences for the uplink of a DS-CDMA system in frequency selective fading channels," in *Global Telecommunications Conference*, vol. 4, pp. 1867-1871, December 2003.

- [42] J. Thomas and T. Cover, *Elements of Information Theory*, NewYork: Wiley, 1991.
- [43] R. G. Gallager, *Information Theory and Relaiable Communication*, NewYork: Wiley, 1968.
- [44] A. J. Goldsmith and P. P. Varaiya, "Capacity, mutual information and coding for finite state Markov channels," *IEEE Transactions on Information Theory*, vol. 42, no. 3, pp. 868-886, May 1996.
- [45] V. Sharma and S. K. Singh, "Maximum likelihood sequence estimation in channels with intersymbol interference and noise memory," in *Proceedings of IEEE International Symposium of Information Theory*, pp. 366-366, August 1998.
- [46] D. M. Arnold and H. A. Loeliger, "On the information rate of binary- input channels with memory," in *Proceedings IEEE International Conference on Communications*, pp. 2692-2695, June 2001
- [47] H. D. Pifster, J. B. Soriaga, and P. H. Siegel, "On the achievable information rates of finite state ISI channels," in *Proceedings IEEE Global Telecommunications Conference*, Dallas, TX, , pp. 2992-2996, November 2001.
- [48] X. Ma, N. Varnica, and A. Kavcic, "Matched information rate codes for binary ISI channels," in *Proceedings IEEE Int. Symp. Information Theory*, Lausanne, Switzerland, pp. 269-269, June 2002.
- [49] L. C. Barbosa, "Simultaneous detection of readback signals from interfering-magnetic recording tracks using array heads," *IEEE Transactions on Magnetics*, vol. 26, no. 5, pp. 2163-2165, September 1990.

- [50] P. A. Voois, J. M. Cioffi, "Multichannel digital magnetic recording communications," *IEEE International Conference on Communications*, vol. 1, pp. 125-130, June 1992.
- [51] D. N. Dung and Krishna R. Narayanan, "Design of good low-rate coding schemes for ISI channels based on spectral shaping," *IEEE Transactions on Wireless Communications*, vol. 4, no. 5, pp. 2309-2317, September 2005.
- [52] R. Raheli, A. Polydoros, and C. Tzou, "Per-survivor processing: A general approach to MLSE in uncertain environments," *IEEE Transactions on Communications*, vol. 43, pp. 354-364, Feb./Mar./Apr. 1995.

APPENDIX A

THE DERIVATION OF THE SUM CAPACITY LOSS FOR TWO-TRACK MAGNETIC RECORDING SYSTEM WHEN THE SIGNALS OF THE TWO TRACKS ARE COMBINED

According to the section A, Chapter VI, the read signals from the two-magnetic read heads are given by

$$y_1(D) = (x_1(D) + \alpha x_2(D))h(D) + n_1(D), \quad (\text{A.1})$$

$$y_2(D) = (x_2(D) + \alpha x_1(D))h(D) + n_2(D). \quad (\text{A.2})$$

Here, we assume that N symbols are read from each track. Taking N length Fourier transform of the signals read from the two heads

$$Y_{1,k} = H_k X_{1,k} + \alpha H_k X_{2,k} + N_{1,k}, \quad (\text{A.3})$$

$$Y_{2,k} = H_k X_{2,k} + \alpha H_k X_{1,k} + N_{2,k}. \quad (\text{A.4})$$

Here, H_k is the frequency spectrum of the channel at the k th frequency index. Since we are considering the symmetric capacity of the channel, we assume that $E[|X_{1,k}|^2] = E[|X_{2,k}|^2] = p_k$. Where, p_k is the each read head's signal power at the k th subcarrier. The capacity of the system at the k th subcarrier is given by

$$C_k = h(Y_{1,k}, Y_{2,k}) - h(Y_{1,k}, Y_{2,k} | X_{1,k}, X_{2,k}, H_k). \quad (\text{A.5})$$

At low SNR region, the effect of the noise dominates and we can assume that $h(Y_{1,k}, Y_{2,k})$ is jointly Gaussian. Hence, the capacity of the system at the k th subcarrier is given by

$$C = \frac{1}{2} \log(|I_2 + \frac{p_k}{\sigma^2} \mathbf{H}_k \mathbf{H}_k^H|) \quad (\text{A.6})$$

where

$$\mathbf{H}_k = \begin{bmatrix} 1 & \alpha \\ \alpha & 1 \end{bmatrix} H_k. \quad (\text{A.7})$$

The sum capacity is given by $C_k = \frac{1}{2} \log(|I_2 + \frac{p_k}{\sigma^2} \mathbf{H}_k \mathbf{H}_k^H|)$ can be simplified as

$$C_k = \frac{1}{2} \log(1 + 2H_k^2 \frac{p_k}{\sigma^2} (1 + \alpha^2) + H_k^2 (\frac{p_k}{\sigma^2})^2 (1 + \alpha^2)^2 - 4H_k^2 (\frac{p_k}{\sigma^2})^2 \alpha^2) \quad (\text{A.8})$$

As $SNR \rightarrow 0$, we can further simplify the formula and get

$$C = \frac{Q}{\sigma^2} (1 + \alpha^2) \quad (\text{A.9})$$

where $Q = \sum H_k^2 p_k$. Now, if we simply combine the channels in (6.1) we get an equivalent channel as

$$Y_k = (1 + \alpha)(X_{1,k} + X_{2,k})H_k^2 + N_k. \quad (\text{A.10})$$

Here, the variance of the noise N_k will be $2\sigma^2$. The capacity of the combined channel at the k th subcarrier, can be shown as

$$C_{k,combined} = \frac{1}{2} \log(1 + H_k^2 \frac{p_k}{\sigma^2} (1 + \alpha)^2) = \frac{p_k}{2\sigma^2} (1 + \alpha)^2 \quad (\text{A.11})$$

The capacity of the combined channel is given by

$$C_{combined} = \frac{Q}{2\sigma^2} (1 + \alpha)^2. \quad (\text{A.12})$$

Hence, the fractional capacity loss $\frac{C - C_{combined}}{C}$ is given by

$$\kappa = (1 - \alpha)^2 / (2(1 + \alpha^2)). \quad (\text{A.13})$$

VITA

Bemini Hennadige Janath Peiris was born in Galle, Sri Lanka. He received a B.Sc. (Eng.) degree in electronics and telecommunications from the University of Moratuwa, Sri Lanka in 1997, a M.Eng. degree in telecommunications from the Asian Institute of Technology, Thailand in 2000, and a Ph.D. degree at Texas A&M University, in electrical engineering in 2006. From 1997 to 1999, he was a lecturer with the Department of Electronic and Telecommunications at the University of Moratuwa. In summer 2000, he was a visiting researcher at the University of Ferrara, Italy. In spring 2005, he was a visiting scholar at the Institute of Eurecom Sophia Antipolis, France. In Fall 2005, he worked as an intern at Qualcomm Inc. in San Diego. His research interests include OFDM, spread spectrum CDMA, and error control coding. His permanent address is 95-1-6, Bandaranayake Mawatha, Indigolla, Gampaha, Western Province, Sri Lanka. He can be contacted through email: janath.peiris@gmail.com